

RESEARCH MEMORANDUM

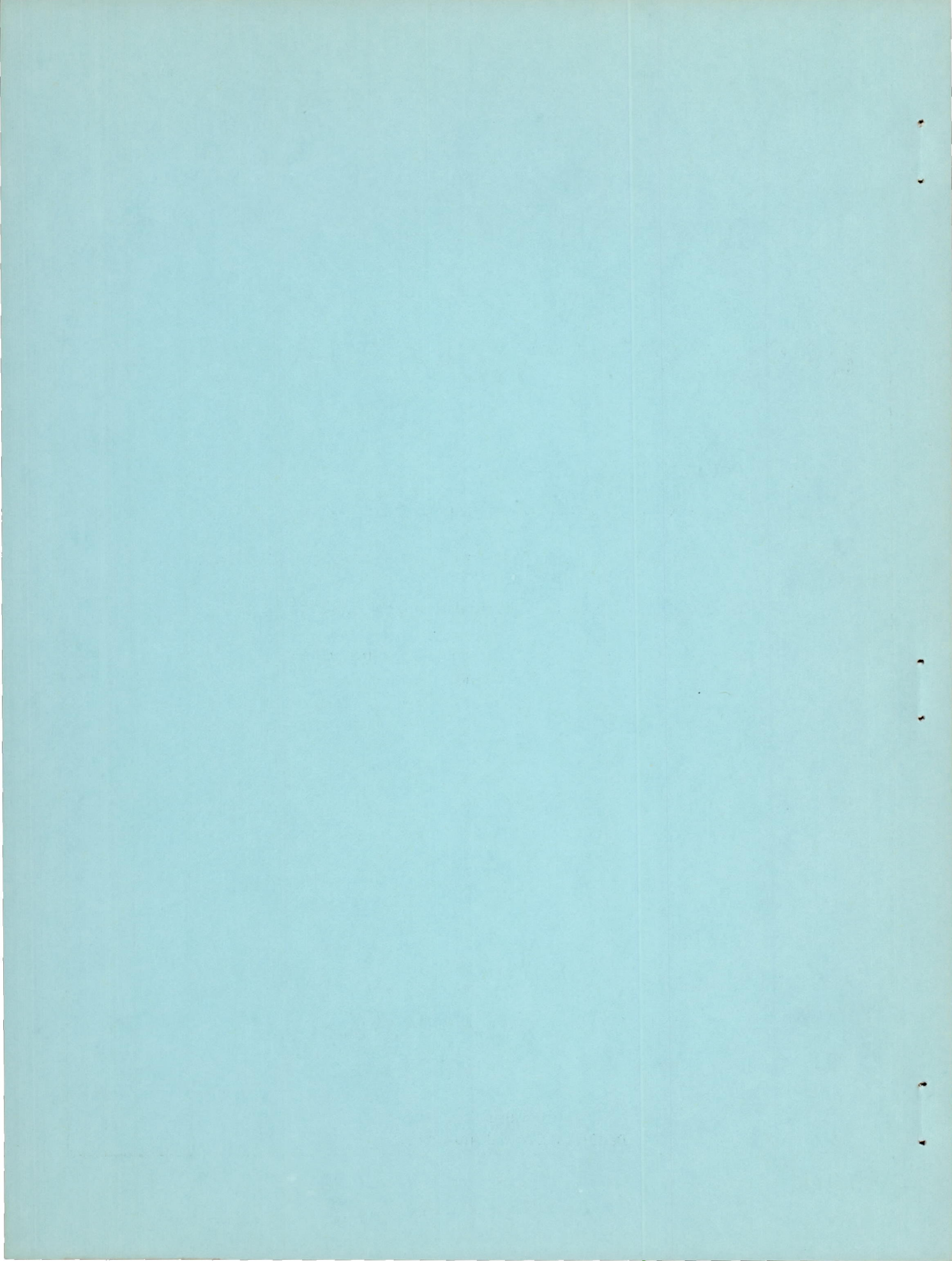
INVESTIGATION OF LIQUID FLUORINE AND HYDRAZINE-AMMONIA
MIXTURE IN 100-POUND-THRUST ROCKET ENGINE

By Paul M. Ordin, Edward A. Rothenberg, and William H. Rowe

Lewis Flight Propulsion Laboratory
Cleveland, Ohio

NATIONAL ADVISORY COMMITTEE
FOR AERONAUTICS
WASHINGTON

October 29, 1952
Declassified January 12, 1961



NATIONAL ADVISORY COMMITTEE FOR AERONAUTICS

RESEARCH MEMORANDUMINVESTIGATION OF LIQUID FLUORINE AND HYDRAZINE-AMMONIA MIXTURE
IN 100-POUND-THRUST ROCKET ENGINE

By Paul M. Ordin, Edward A. Rothenberg, and William H. Rowe

SUMMARY

Specific impulse, characteristic velocity, thrust coefficient, and heat rejection of liquid fluorine and a fuel consisting of a hydrazine-ammonia mixture were determined for a range of fuel percentages (fuel to total propellant flow) in a 100-pound-thrust rocket engine designed for a combustion-chamber pressure of 300 pounds per square inch absolute. The fuel consisted of 59 percent hydrazine, 37 percent ammonia, and 4 percent water.

The maximum experimental specific impulse was 277 pound-seconds per pound (88 percent of the theoretical value) at 37 weight percent fuel and was obtained with a one fuel - one oxidant impinging-jet injector in a 50 L* engine. When a turbulence coil was placed in front of the injector, the performance was increased over the range of 17 to 35 weight percent fuel but the maximum performance was 276 pound-seconds per pound at 33 weight percent fuel. The correction for the heat rejection and for deviations from the reference combustion-chamber pressure raised the specific impulse obtained with the one fuel - one oxidant impinging-jet injector with a turbulence coil to 284 pound-seconds per pound, approximately 94 percent of the theoretical value for the nozzle and fuel used. The specific impulse for the one fuel - one oxidant impinging-jet injector without the turbulence coil was increased to 282 pound-seconds per pound by the corrections.

The experimental characteristic velocity with the one fuel - one oxidant impinging-jet injector reached a maximum of 6690 feet per second (94 percent of the theoretical value) at 34 weight percent fuel. The experimental characteristic velocity with the one fuel - one oxidant impinging-jet injector with turbulence coil was increased over the entire fuel-oxidant range with a maximum of 6820 feet per second (96 percent of the theoretical value) at 33 weight percent fuel. The maximum experimental thrust coefficient obtained from the curve drawn through all the experimental points was 1.30, 92 percent of the theoretical value. Heat rejection values from 2.0 to 3.6 Btu per second per square inch were obtained for the 50 L* engine with the impinging-jet turbulence injector and values from 2.0 to 2.5 Btu per second per square inch with the impinging-jet injector.

The performance obtained with a 100 L* engine with a shower-head-type injector fitted with a turbulence grid was within 4 percent of that obtained with the impinging-jet turbulence coil injector, while the heat

rejection was approximately 20 percent lower. No difficulties were experienced with solid deposits in the engine during the investigation.

INTRODUCTION

It is generally agreed that the desirability of using liquid fluorine as a rocket oxidant is limited to long-range missiles in which high specific impulse and high bulk densities are prime factors in reducing missile weight or increasing range. Satisfactory techniques for the handling of liquid fluorine have been developed which indicate that the loading of a missile with liquid fluorine will not be particularly difficult.

Maximum theoretical specific impulse values, based on equilibrium expansion from a combustion-chamber pressure of 300 pounds per square inch absolute for liquid fluorine and liquid oxygen with various fuels are:

Fuel Oxidant	Hydrogen H ₂	Lithium Li	Hydrazine N ₂ H ₄	60 percent N ₂ H ₄ 40 percent NH ₃	Ammonia NH ₃	Diborane B ₂ H ₆
Fluorine	364	^a 335	315	313	312	^b 311
Oxygen	^c 349	^c 318 (Frozen expansion)	^c 270	^d 263	257	299

^aReference 1.

^bReference 2.

^cReference 3.

^dReference 4.

The experimental evaluation of the performance of liquid fluorine with several of the fuels listed is being conducted at the NACA Lewis laboratory. The results obtained with liquid fluorine and liquid diborane are presented in reference 2. Other fuels of interest are ammonia, hydrazine, mixtures of ammonia in hydrazine, and liquid hydrogen. The fuel selected for the experimental investigation reported herein was a 37-weight-percent solution of ammonia in hydrazine; the selection was based on a compromise requirement of physical and performance properties between liquid ammonia and hydrazine. The advantages of liquid ammonia as a rocket fuel are its availability, low cost, and low freezing point whereas the disadvantages include high vapor pressure, lower density, and slightly lower performance. Hydrazine as a rocket fuel has the advantages of higher density, lower vapor pressure, and higher performance with the disadvantages of a comparatively high freezing point, low availability, and high cost. A list of the properties of liquid fluorine, ammonia, hydrazine, and a mixture of 37-weight-percent ammonia in hydrazine is given in table I. A mixture of 38-weight-percent ammonia in hydrazine is homogeneous with a melting point of -37.5°C .

The investigation reported herein was conducted at the NACA Lewis laboratory with a 100-pound-thrust rocket engine at a combustion-chamber pressure of 300 pounds per square inch absolute. Experimental values were determined for specific impulse, characteristic velocity, thrust coefficient, and heat rejection for a range of fuel percentages. The

propellant injection methods were varied during the investigation in order to obtain experimental performance comparable to the theoretical values. The effects of the injection system on the specific impulse, characteristic velocity, and heat transfer were observed. In addition, the characteristic engine length was varied from 50 to 100 inches and its effect on the performance was observed.

SYMBOLS

The following symbols are used in this report:

A_t	exhaust-nozzle throat area, sq in. or sq ft
A_t/W	throat area per unit flow rate, sq ft/lb/sec
a_t	velocity of sound at throat, ft/sec
C^*	characteristic velocity, $P_c A_t g/W_0 + W_f$, ft/sec
C_F	thrust coefficient, $F/P_c A_t$
F	engine thrust, lb
g	gravitational constant, 32.17 ft/sec ²
I	theoretical specific impulse
I_{corr}	experimental specific impulse of rocket engine corrected for heat rejection, lb-sec/lb
I_{exp}	experimental specific impulse of rocket engine, $F/W_0 + W_f$, lb-sec/lb
J	mechanical equivalent of heat, 778 ft-lb/Btu
K	rate of change of specific impulse with combustion-chamber pressure, $\frac{\text{lb-sec/lb}}{\text{lb/sq in. abs}}$
L^*	characteristic length, ratio of combustion-chamber volume to nozzle throat area, in.
M_t	mean molecular weight at nozzle throat, g/mol
P_c	combustion-chamber pressure, lb/sq in. abs or atm
P_t	pressure at nozzle throat, lb/sq in. or atm

Q	heat rejection per unit propellant weight, Btu/lb
T_c	theoretical chamber temperature, °K
T_e	theoretical exit temperature, °K
T_t	theoretical temperature at nozzle throat, °K
W_f	fuel flow, lb/sec
W_o	oxidant flow, lb/sec
β	resultant angle of impinging jets with respect to engine axis
ΔI_p	change in specific impulse with chamber pressure
η	ideal thermodynamic cycle efficiency, $1 - T_e/T_c$

PROPELLANTS

Gaseous fluorine was obtained from an industrial supplier in commercial gas cylinders. Each cylinder contained about 6 pounds of 98-percent-pure fluorine under a pressure of approximately 360 pounds per square inch absolute. The fluorine gas was condensed in a nickel tank that was immersed in a liquid nitrogen bath.

The fuel used was a mixture of 59 percent hydrazine, 37 percent ammonia, and 4 percent water. The mixture was prepared by introducing a weighed amount of commercial hydrazine into a mixing tank. The required amount of ammonia was then bubbled through the hydrazine. The mixing tank was vigorously agitated, then allowed to stand for several days in order to obtain a uniform mixture. The composition of the mixture was based on the weighed quantities of ammonia and hydrazine. The freezing point of the mixture was found to be -34° C as compared with a previously published value of -37.5° C for a mixture containing 57.04 percent hydrazine, 38.0 percent ammonia, and 4.96 percent water (reference 4).

APPARATUS

A complete flow diagram of the apparatus used throughout the investigation is shown in figure 1. Helium, controlled by two-stage pressure regulation, was used to drive the propellants into the combustion chamber. The pressurizing helium was cooled in a liquid-nitrogen bath before entering the fluorine supply tank.

2671

The fluorine flow system was made up entirely of nickel or monel tubing and brass fittings. The fluorine flow lines and hand valves were jacketed to permit cooling with liquid nitrogen. The liquid-fluorine supply tank, immersed in a constant-level liquid-nitrogen bath, was suspended from a cantilever weighing beam. A photograph of the fluorine supply system is shown in figure 2. Remote and hand operated valves in the fluorine system were of the commercial refrigeration type, packless and with copper-monel seats. Figure 3 is a diagrammatic sketch of the remote operating mechanism used for the flow-control valves in the fluorine system.

A closed system was used to transfer the hydrazine-ammonia mixture from the mixing tank to the supply tank. The supply tank was suspended from one side of a chemical balance beam. Enough weight was put on the other side of the beam to just counterbalance the weight of the empty fuel tank. Stainless-steel lines, fittings, and valves were used to carry the fuel to the rocket engine.

The thrust stand was a bearing-type pivoted stand with the engine mounted at a downward angle of 30° on the end of one lever arm with the second lever arm, of equal length, attached to a cantilever beam. A photograph of the thrust stand with a rocket mounted is shown in figure 4.

The engine assembly consisted of two units, a water-cooled combustion chamber with a nozzle and a propellant injector. The rocket engines were designed to deliver 100-pounds thrust at a combustion-chamber pressure of 300 pounds per square inch absolute. The combustion chambers had characteristic lengths of 50 and 100 inches.

Both the combustion chamber and nozzle were made of either nickel or brass and were designed for either annular or spiral coolant passages. A dimensional sketch and a photograph of the nickel annular cooled chamber are shown in figure 5. The combustion chamber and nozzle for the brass engine were designed to permit 0.004-inch nickel plating. The plating was not adherent, and for the several runs made the value of the throat diameter used in the calculations was 0.561 inch. A pressurized supply tank provided water at a flow rate of 5 to 10 pounds per second, which was sufficient to cool the engine. A coolant velocity of approximately 100 feet per second was maintained at the nozzle throat section.

The performance of a number of different injectors was studied. A shower-head type injector was used which had 22 fuel holes and 66 oxidant holes (fig. 6). The shower-head injector was modified by forming a water-cooled grid of 3/16-inch copper tubing and mounting it approximately 5/8 inch from the injector face (fig. 7). An impinging-jet injector consisting of one fuel jet on one oxidant jet with eight pairs of holes (1-1 injector) was also used (fig. 8). This injector was

modified also by the addition of a turbulence coil. The impinging-jet injector with the water-cooled coil of 3/16-inch copper tubing is shown in figure 9 (coil A). This coil was later modified slightly to place the first coil turn approximately 1/8 inch beyond the impingement point of the propellant jets (coil B). An impinging-jet injector consisting of six sets of holes each with two oxidant jets impinging on one fuel jet was investigated. It was later modified by the addition of a deflector plate to direct the oxidant flow across the inner face of the injector. The two oxidant - one fuel impinging-jet injectors are shown in figure 10.

INSTRUMENTATION

Propellant flow. - The propellant tanks were suspended from cantilever beams to which strain gages had been cemented. The strain gages were connected in resistance bridge circuits and changes in weight were recorded as voltage changes on a recording, self-balancing potentiometer. Matching units permitted full-scale chart readings for three different weight ranges. A full-scale reading could be obtained at 1, 2, and 4 pounds in the fuel system, and 5, 10, and 15 pounds in the fluorine system.

Dead-weight calibrations on both the fuel and oxidant systems were made before and after each run. The dead-weight constants were obtained by recording the number of chart spaces per unit of applied weight. The average variation in dead-weight constant throughout the entire program for the fuel and oxidant systems was ± 0.6 percent. The precision of flow measurements for the fuel system was 1.1 percent and for the oxidant system 1.2 percent.

Thrust measurement. - Thrust was measured by a strain gage mounted on a cantilever beam and recorded through a resistance-bridge circuit on a recording, self-balancing potentiometer. A matching unit provided a variation of the full-scale range. Full chart scale could be obtained at 50, 100, or 200 pounds force.

Thrust was determined from the average of dead-weight calibrations made before and after each run. These calibrations were made without engine coolant-water flow; calibrations made with the engine coolant water were within 1 percent of the values obtained without the coolant water. The average variation of the dead weight constant throughout the entire program was ± 1.3 percent. The reproducibility of the experimentally determined thrust, including the variations due to dead-weight constant and chart reading was within 1.7 percent.

Pressure and temperature. - Propellant- and coolant-injection pressure and combustion-chamber pressure were measured by Bourdon tube-type pressure gages. The gages were photographed at a rate of 4 frames per second during a run. Chamber pressure was also measured by a Bourdon-tube pressure recorder.

Copper-constantan and iron-constantan thermocouples, the outputs of which were recorded on self-balancing potentiometers, were used to measure propellant-injection temperatures; engine coolant-water inlet and outlet temperatures, and coil coolant-water inlet and outlet temperatures. Temperature readings are accurate to within 1 percent.

Coolant flow. - The engine coolant-water flow was measured by a variable-area orifice meter equipped with an electric transmitter and recorder. The accuracy of this measurement was within 2 percent.

The coil coolant-water flow was obtained by plotting water flow against the pressure on the coolant supply tank. The water flow was determined by weighing the water flowing through the coil over a given time interval.

PROCEDURE

Operations. - Prior to the firing of the rocket engine, all valves and fittings were pressure checked. The entire propellant flow system was then purged with helium. The hydrazine-ammonia mixture was loaded through a closed system directly into the fuel-supply tank. The fluorine cylinder was opened remotely (fig. 2) and gaseous fluorine was condensed in the liquid-nitrogen-cooled fluorine-supply tank.

The propellant-supply tanks were pressurized from a remote position. Liquid nitrogen was passed through the fluorine flow lines until the lines were at the liquid-nitrogen temperature; the nitrogen flow was stopped and the fluorine flow valve opened; immediately thereafter the fuel flow valve was opened. Ignition was spontaneous. After the run, 15 to 30 seconds duration, both propellant systems were purged with helium. A helium atmosphere, under about 150 pounds per square inch pressure, was maintained in the propellant tanks until the next run.

Data presentation. - The specific impulse was calculated from the measured thrust and propellant flow rates. For adiabatic comparisons with theoretical data, the specific impulse values were corrected for total heat rejection to the combustion-chamber walls and turbulence coil. The heat rejection was taken as the product of the specific heat of water, the coolant flow rate, and the temperature difference between the inlet and outlet coolant water. The impulse correction used was a function of the ideal thermodynamic cycle efficiency and the calculated total heat rejection and is given by the equation

$$I_{\text{corr}} = \sqrt{I_{\text{exp}}^2 + \frac{2JQ\eta}{g}}$$

An additional correction was applied for any variation of chamber pressure from a base of 300 pounds per square inch absolute. This correction, based on the theoretical increase of specific impulse with combustion-chamber pressure at optimum area ratios, is approximated by the equation

$$\Delta I_p \cong K \log (p/P_c)$$

where P_c is 300 pounds per square inch absolute, p is the experimental value of the combustion-chamber pressure, and K is 88.65 (fig. 11).

The pressure corrections were less than 2.5 percent of the experimental specific impulse for the seven runs which had combustion-chamber pressures less than 285 and greater than 315 pounds per square inch and less than 1 percent for the remainder of the runs.

Theoretical calculations indicate that for the nozzle used, the contribution of the pressure thrust was only 1 percent of the increased total thrust in increasing the combustion-chamber pressure from 300 to 350 pounds per square inch. The increase in specific impulse obtainable with an increase in combustion-chamber pressure is almost entirely caused by the increase in pressure-expansion ratio through the nozzle (reference 6).

Characteristic velocity and thrust coefficient were also calculated from experimentally determined values of combustion-chamber pressure, propellant flow rate, and thrust. The theoretical characteristic velocity was calculated from the expression

$$C^* = gP_c \frac{A_t}{W}$$

where the throat area per unit flow rate was obtained from the continuity equation

$$\left(\frac{A_t}{W} \right)_{\text{equil}} = \frac{1.3144 (T_t)}{P_t M_t a_t}$$

The velocity of sound and the nozzle throat conditions for equilibrium composition were determined by the method described in reference 1 rather than by the conventional method of using the specific-heat ratios. The theoretical thrust coefficient was obtained from the equation

$$C_F = \frac{I_g}{C^*}$$

RESULTS AND DISCUSSION

Specific impulse. - A compilation of the experimental data is given in table II. The experimental specific impulse is shown in figure 12 for a propellant mixture range of 16 to 44 weight percent fuel; the theoretical curve based on equilibrium composition expansion is also shown for comparison. Curves are drawn through the experimental points obtained with the 50 L* engine using the 1-1 impinging-jet injector, 1-1 impinging-jet injector with turbulence coil, and shower-head-type injector. The curve drawn through the points obtained with the 1-1 impinging-jet injector with turbulence coil gave the maximum results in the region from 17 to 35 weight percent fuel, following the theoretical curve within 80 to 90 percent. (The theoretical values were calculated by the method described in reference 6.) The maximum experimental value for this configuration was 276 pound-seconds per pound and was obtained at 33 weight percent fuel. The maximum theoretical specific impulse of 313 pound-seconds per pound is at 28 percent fuel; the stoichiometric ratio is 26.8 percent.

Specific impulse values obtained with the 50 L* engine and 1-1 impinging-jet injector were lower in the region of 17 to 35 percent fuel than those obtained when the turbulence coil was used. In the region greater than 35 weight percent fuel, however, the experimental performance with the use of the 1-1 impinging-jet injector without the turbulence coil was slightly higher than with the coil. The maximum experimental value of 277 pound-seconds per pound at 37 percent fuel was obtained with the 1-1 impinging-jet injector. Since ammonia can be considered as a coolant, the greater performance obtained in the fuel-rich region is desirable. The use of a more efficiently designed turbulence coil would probably have given even higher performance. Two runs made with the L* of the engine increased to 100 and the impinging-jet injector gave no increase in performance. The performance obtained with the shower-head-type injector and the 50 L* engine was extremely low throughout the fuel-oxidant range investigated. A maximum experimental value of 223 pound-seconds per pound was obtained at 38 percent fuel. When the L* of the engine was increased from 50 to 100, the performance, indicated by the one run with the shower-head injector, increased from 220 pound-seconds per pound to 246 pound-seconds per pound at about 34 percent fuel. The maximum specific impulse obtained with the 100 L* engine and shower-head injector fitted with a grid-type turbulence coil was 266 pound-seconds per pound as compared with 276 pound-seconds per pound obtained with the 1-1 impinging-jet turbulence injector in the 50 L* engine.

The theoretical curve corrected for nonparallel flow and for the composition of the fuel, and the experimental curves corrected for heat rejection and for deviations from the reference combustion-chamber pressure of 300 pounds per square inch absolute are shown in figure 12(b). The theoretical curve is lowered a total of approximately 4 percent because of the 30° divergent angle of the exhaust nozzle and the 4 percent water in the fuel. The corrected theoretical curve indicates a maximum of 301 pound-seconds per pound at 28 percent fuel. In a comparison of figures 12(a) and 12(b), it can be seen that the experimental curve

obtained with the 1-1 impinging-jet injector with turbulence coil is raised by the corrections approximately 7 percent in the oxidant-rich region (17 to 25 weight percent fuel) and about 4 percent in the region from 25 to 40 weight percent fuel. The maximum value of 284 pound-seconds per pound was obtained at 33 percent fuel (94 percent of the theoretical value, corrected). The experimental values obtained with the 1-1 impinging-jet injector are raised approximately 4 percent in the region from 17 to 25 weight percent fuel; and about 2 percent from 25 to 40 weight percent fuel. The corrected experimental curves for the 1-1 impinging-jet injector with and without turbulence coil are the same in the region greater than 35 weight percent fuel. The experimental values obtained with the shower head and shower head with grid injector are raised approximately 3 percent by the addition of the heat-rejection corrections. The maximum specific impulse of the 100 L* engine with the shower head with injector grid increased to 274 pound-seconds per pound (91 percent of the theoretical value, corrected).

These results indicate that in spite of the high reactivity of fluorine, engines using this oxidizer require a critically designed injector for high performance. The difference in specific impulse values obtained with the impinging-jet injectors with and without turbulence coils (fig. 12) indicates the importance of providing some means of increasing the mixing and residence time of the propellants in the rocket chamber. An increase of approximately 3 to 13 percent in specific impulse in the region of 20 to 33 weight percent fuel was obtained with the use of the turbulence coil. In the region from 36 to 43 percent fuel, the results from the impinging-jet injector are slightly greater. Beyond 36 percent fuel, the coil no longer contributes to the mixing of the propellants and the lower performance is a result of the heat loss to the coil (see table II). The location of the coil with respect to the injector is important. The coil shown in figure 9 resulted in approximately the same performance as the injector without the coil. However, the modified coil with the initial turn $1/8$ inch from the impingement point of the jets (coil B) resulted in the increased performance shown in figure 12.

The modified arrangement did not give superior performance over the entire range. This can be explained by the following analysis. The impinging-jet injectors as shown in figure 8 were designed with the oxidant flow entering the chamber axially while the fuel entered at a 60° angle. The resultant stream was directed inward towards the center of the engine at an angle which increased with greater fuel flows. A plot of the resultant angle of momentum against the weight percent fuel is shown in figure 13. At weight percent fuels greater than 36, the angle of the resultant stream was sufficiently large to miss the turbulence coil, thus resulting in no increase in performance over the plain impinging-jet injector. The use of an impinging-jet turbulence coil configuration which will cause the impingement of the resultant propellant stream with the coil throughout the complete fuel-oxidant range will no doubt increase the performance throughout that range.

The results obtained with the shower-head-type injector indicate again the importance of providing sufficient mixing and residence time for the fluorine and hydrazine-ammonia propellant combination. In the 50 L* engine, the performance remained extremely low; increasing the L* from 50 to 100 to provide greater residence time increased the performance approximately 10 percent. In order to further increase the performance, a copper grid (fig. 7) was provided to promote better mixing of the propellants. The results obtained with the grid and shower-head injector combination with the 100 L* engine approached within 4 percent of the performance obtained with the impinging-jet turbulence injector and 50 L* engine.

Characteristic velocity. - The effect of the injection system on the characteristic velocity is, of course, similar to the effect on specific impulse as shown in figure 14. The experimental curves are drawn through the points obtained in the 50 L* engine with the three injectors: 1-1 impinging-jet injector with turbulence coil, 1-1 impinging-jet injector, and shower-head-type injector. Maximum values of C* were obtained with the 1-1 impinging-jet injector with turbulence coil. The peak value of 6820 feet per second was obtained at 33 weight percent fuel, which compares favorably with the theoretical maximum of 7080 feet per second at 31 weight percent fuel. In the region from 22 to 40 percent fuel, experimental values from 90 to 96 percent of the ideal theoretical values were obtained.

The values of C* obtained with the 1-1 impinging-jet injector were lower in the region from 17 to 37 weight percent fuel than those obtained when the turbulence coil was used; however, similar values for the two injectors were obtained at fuel percentages greater than 37 percent. The two runs made with the use of the impinging-jet injector and 100 L* engine gave no increase in performance. The values of C* for the shower-head injector and 50 L* engine were low throughout the fuel-oxidant range investigated. The use of the shower-head injector with the 100 L* engine resulted in an increase in performance from about 5820 to 6260 feet per second at 34 percent fuel. The results of the three runs with the turbulence grid placed in front of the shower-head injector of the 100 L* engine were within 2 percent of the values obtained with the impinging-jet turbulence injector in the 50 L* engine. The peak value obtained was 6710 feet per second at 35 weight percent fuel.

Maximum experimental values of C* from 92 to 96 percent of the theoretical values were obtained as compared with the 80 to 90 for the specific impulse and 88 to 92 for the thrust coefficient.

A plot of the thrust coefficient C_F against weight percent fuel is shown in figure 15. The maximum experimental value of C_F obtained was 1.30 at 32 weight percent fuel, which compared with the theoretically

calculated value of 1.42. Measurements of the engine-throat diameter, which were taken immediately after running, indicated no change. The deviation of the experimental values of C_F from the theoretical values may be due to the nozzle divergence and heat transfer to the nozzle wall which could result in nonideal equilibrium conditions.

Heat rejection. - The values of heat rejection in Btu per second per square inch against weight percent fuel for the engine configurations used are shown in figure 16(a). The heat rejection to the coil of the impinging-jet-turbulence injector remained constant at approximately 4 Btu per second per square inch from 17 to 30 weight percent fuel and decreased to approximately 2.5 Btu per second per square inch at 39 percent fuel. The low values of heat rejection occurred at fuel percentages greater than 36 percent, the value at which the resultant propellant streams missed the turbulence coil. Heat rejections of 2.5 to 3.4 Btu per second per square inch were obtained from the 50 L* engine in which the impinging-jet turbulence coil injector was used. Lower values of heat rejection, from 2.0 to 2.5 Btu per second per square inch were obtained for the 50 L* engine in which the 1-1 impinging-jet injector was used.

The heat rejections to the 50 L* engine in which the shower-head injector was used were less than 1 Btu per second per square inch. The total heat rejections to the impinging-jet turbulence coil injector with the 50 L* engine and shower head with grid with the 100 L* engine are given in figure 16(b); also included are the theoretical chamber temperatures. The total heat rejection for the impinging-jet turbulence coil with the 50 L* engine configuration varied from 3.6 at 20 percent fuel to 2.0 Btu per second per square inch at 43 percent fuel. The total heat rejection for the shower head with grid with the 100 L* engine configuration as drawn through the three experimental points varied from 2 Btu per second per square inch at 16 percent fuel to 2.4 Btu per second per square inch at 35 percent fuel. The heat rejection obtained with the shower-head with grid with the 100 L* engine was almost 20 percent lower than that of the impinging-jet turbulence coil with the 50 L* engine while the maximum experimental specific impulse value was within 4 percent. These preliminary results with the shower-head with grid injector and the 100 L* engine indicate that additional studies of such a configuration may be warranted in an effort to obtain high performance with minimum cooling requirements.

The theoretical chamber temperature increased from 3320° K at 16 percent fuel to a maximum of 4380° K at 26 percent fuel. The exit temperature calculated for equilibrium composition increased from 1540° K at 16 percent fuel to a maximum of 3160° K at 27 percent fuel.

T105

The only injector burnouts experienced were with an impinging-jet injector consisting of two oxidant jets impinging on one fuel jet (fig. 10). Two runs were made but in each case the injector burned within the first three seconds of operation. The burning was initiated in the center portion of the injector. In an attempt to eliminate the burning of the two oxidant - one fuel impinging-jet injector, a deflector plate was introduced behind the center portion of the injector face to provide for more efficient cooling of the surface (fig. 10). One run was made with this injector but a burnout resulted within the first two seconds of operation.

Solid deposits of ammonium fluoride on the combustion-chamber walls were noticed when the fuel flow into the combustion chamber continued after the fluorine flow appeared to be over. The deposits caused no difficulty in the operation of the engine.

SUMMARY OF RESULTS

The theoretical performance of the liquid fluorine, 40 percent ammonia, and 60 percent hydrazine propellant combination was calculated and experiments were conducted to determine the performance of the combinations in a 100-pound-thrust rocket engine at a combustion-chamber pressure of 300 pounds per square inch absolute. The investigation produced the following results:

1. The peak specific impulse with the impinging-jet injector and 50 L* engine was 277 pound-seconds per pound at 37 weight percent fuel. The use of a turbulence coil with the 1-1 impinging-jet injector in a 50 L* engine resulted in higher specific impulse values in the region of 17 to 35 weight percent fuel (where resultant propellant streams impinged on the coil) than the values obtained with the impinging-jet injector without a coil. The maximum specific impulse with the impinging-jet turbulence injector was 276 pound-seconds per pound and was obtained at 33 weight percent fuel.
2. The maximum specific impulse with the impinging-jet turbulence coil injector increased to approximately 284 pound-seconds per pound when corrected for the heat loss and small deviations of the combustion-chamber pressure from 300 pounds per square inch absolute. This value is 94 percent of the maximum theoretical specific impulse for the fuel and nozzle used. The specific impulse for the impinging-jet injector without the turbulence coil was increased to 282 pound-seconds per pound by the corrections.
3. Runs made with the 50 L* engine with a shower-head injector indicated low performance throughout the fuel-oxidant range investigated. Increasing the mixing and residence time of the propellants with the shower-head injector by increasing the characteristic length from 50 to 100 inches and installing a turbulence grid resulted in an increase of approximately 15 percent in performance.

4. The experimental characteristic velocity with the impinging-jet turbulence injector and 50 L* engine reached a maximum of 6820 feet per second at 33 weight percent fuel. The theoretical value of 7090 feet per second was obtained at 31 weight percent fuel.

5. The experimental thrust coefficient averaged 1.30 as compared with the theoretical value of 1.42.

6. The heat rejection to the engine configuration consisting of the impinging-jet turbulence injector and the 50 L* engine varied from 2.0 to 3.6 Btu per second per square inch. The heat rejection to the impinging-jet injector and 50 L* engine varied from 2.0 to 2.5 Btu per second per square inch.

7. The heat rejection to the shower-head turbulence-grid injector with the 100 L* engine varied from 2.0 to 2.4 Btu per second per square inch; this value was as much as 20 percent lower than that obtained with the impinging-jet turbulence injector and the 50 L* engine while the performance obtained was within 4 percent.

8. Solid deposits of ammonium fluoride were obtained on the combustion-chamber wall but caused no difficulty in the operation of the engine.

CONCLUSION

The attainment of maximum performance with liquid fluorine as the rocket oxidant requires a critical study of injector design in spite of its very high chemical reactivity.

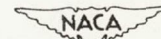
Lewis Flight Propulsion Laboratory
National Advisory Committee for Aeronautics
Cleveland, Ohio

REFERENCES

1. Gordon, Sanford, and Huff, Vearl N.: Theoretical Performance of Lithium and Fluorine as a Rocket Propellant. NACA RM E51C01, 1951.
2. Ordin, Paul M., Douglass, Howard W., and Rowe, William H.: Investigation of the Liquid Fluorine - Liquid Diborane Propellant Combination in a 100-Pound-Thrust Rocket Engine. NACA RM E51I04, 1951.
3. Higbie, H. E., and Rowe, H. E.: Compilation of Propellant Characteristics. Res. and Dev. Rep. No. SPD-262, The M. W. Kellogg Co. for U.S.A.F., Wright-Patterson Air Force Base, March 15, 1950. (Contract No. W-33-038-ac-13916.)

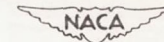
4. Thackrey, James D., Canright, Richard B., and Typaldos, Zissimos A.:
An Exploratory Investigation of Mixtures of Hydrazine and Ammonia
as Rocket Fuels. Prog. Rep. No. 1-69, Power Plant Lab. Proj. MX 801,
Jet Prop. Lab., C.I.T., July 12, 1950. (ORDCIT Proj. Contract
W-04-200-455, Ordnance Dept.)
5. Horvitz, D., and Kircher, H.: Summary Report on Theoretical, Labora-
tory and Experimental Investigation of High Energy Propellants.
Hydrazine as a Rocket Fuel. Vol. 1. Rep. No. RMI-293-S6, Reaction
Motors, Inc., Jan. 14, 1948, to May 5, 1949. (Navy Contract NOa(s)
9469.)
6. Morrell, Virginia E.: Effect of Combustion-Chamber Pressure and
Nozzle Expansion Ratio on Theoretical Performance of Several Rocket
Propellant Systems. NACA RM E50C30, 1950.

TABLE I - PHYSICAL PROPERTIES



	Boiling point (°C)	Melting point (°C)	Density		Critical temperature (°C)	Critical pressure (atm)	Vapor pressure		Specific heat		Heat of vaporization		Reference
			(°C)	(g/cc)			(°C)	(atm)	(°C)	(cal/mole)	(°C)	(kcal/mole)	
Liquid ammonia	-33.4	-77.7	-30 0 20	0.677 .638 .610	132	111.5	-34 0 100 130	0.967 4.238 61.816 106.913	-60 0 20 100	17.799 18.666 19.125 25.16	-33.4	5.56	3
Hydrazine	113.5	1.5	15	1.011	380	145	56 113.5 170 300	0.093 1.0 5.0 56.0	26	23.95	23.1	10.0	3
Ammonia-hydrazine mixture	(36 percent ammonia) -19	(38 percent ammonia) -37.5	(40.1 percent ammonia) -25.0 -7.8 6.0 19.8 33.0	0.888 .872 .856 .842 .828			(36 percent ammonia) 0 14 30 50 70	2.70 4.27 6.75 11.41 18.50					5
Liquid fluorine	-188	-218	-196	1.558	-129	55	-196 -188 -183	0.31 1.00 1.40	-213	10.88	-187.9	1.51	2

TABLE II - SUMMARY OF PERFORMANCE OF LIQUID FLUORINE AND A HYDRAZINE-AMMONIA MIXTURE CONSISTING OF 37 PERCENT AMMONIA, 59 PERCENT HYDRAZINE, AND 4 PERCENT WATER



Run time (sec)	Injector design	Engine characteristic length L*	Fuel flow (lb/sec)	Oxidant flow (lb/sec)	Total propellant flow (lb/sec)	Ratio of fuel weight to total fuel plus oxidant weight	Thrust (lb)	Experimental specific impulse (lb-sec/lb)	Combustion-chamber pressure (lb/sq in. abs)	Total heat rejection (Btu/sec)	Experimental specific impulse corrected (lb-sec/lb)	Experimental characteristic velocity C* (ft/sec)	Experimental thrust coefficient C _F	Heat rejection to engine (Btu/sec)	Heat rejection to coil (Btu/sec)
11	1-1	50	0.09682	0.3593	0.4561	0.2123	94.11	206.3	310	50.11	210.9	5248	1.265	50.11	
18	1-1	50	.09257	.3447	.4373	.2117	94.96	217.2	299	62.78	224.7	5279	1.323	62.78	
19	1-1	50	.1422	.2380	.3802	.3740	105.40	277.2	327	59.90	278.8	6640	1.343	59.90	
19	1-1	50	.1134	.2390	.3524	.3218	91.75	260.4	305	72.41	265.8	6682	1.253	72.41	
23	1-1	50	.1139	.2408	.3547	.3211	94.92	267.6	307	72.00	272.6	6683	1.288	72.30	
27	1-1	50	.1622	.2101	.3723	.4357	87.53	235.1	290	55.70	242.9	6014	1.258	55.70	
26	1-1	50	.1616	.1870	.3486	.4636	84.16	241.4	285	60.71	251.2	6312	1.230	60.71	
22	1-1	50	.1422	.2108	.3530	.4028	85.56	242.4	285	56.81	249.6	6234	1.251	56.81	
13	1-1-CB	50	.0776	.3643	.4419	.1756	85.30	193.0	287	90.72	212.2	5019	1.238	99.98	
22	1-1-CB	50	.1321	.2399	.3720	.3551	102.30	275.0	313	69.20	282.2	6686	1.323	95.20	
21	1-1	100	.1827	.2176	.4003	.4564	96.69	241.5	305	80.20	249.8	6054	1.283	80.20	
20	1-1	100	.1324	.2338	.3662	.3616	98.60	269.3	308	92.23	276.2	6683	1.296	92.23	
16	1-1-CA	50	.0750	.3096	.3846	.1950	87.76	228.2	290	140.50	248.9	5827	1.261	98.50	42.00
24	1-1-CA	50	.03985	.2330	.3649	.3615	98.40	269.7	323	114.20	276.6	6840	1.269	81.50	32.70
22	1-1-CA	50	.0987	.2511	.3498	.2822	95.40	272.7	310	146.50	281.4	6849	1.282	106.00	40.50
13	1-1-CA	50	.0783	.3634	.4417	.1773	89.50	202.6	295	182.60	239.3	5161	1.264	141.50	41.10
22	1-1-CA	50	.1095	.2533	.3628	.3020	95.80	264.0	305	138.65	273.7	6500	1.310	94.75	43.90
17	1-1-CA	50	.1512	.2190	.3702	.4080	94.59	255.5	306	90.40	263.4	6388	1.288	64.80	25.60
26	1-1-CA	50	.1314	.2188	.3502	.3750	94.50	269.8	302	103.30	279.2	6664	1.304	76.50	26.80
23	1-1-CA	50	.0832	.2787	.3619	.2300	89.34	246.9	293	132.10	260.9	6257	1.270	88.10	44.00
11	1-1-CA	50	.0909	.2580	.3490	.2600	92.10	264.0	279	108.00	273.4	6510	1.305	81.40	26.60
26	Shower	50	.1415	.1980	.3395	.4168	75.46	222.3	265	26.74	230.6	6027	1.186	26.74	
12	Shower	50	.09510	.4312	.5263	.1807	101.70	193.2	340	27.85	191.9	4988	1.246	27.85	
13	Shower	50	.1156	.3812	.4968	.2327	99.62	200.5	343	28.96	197.9	5331	1.210	28.96	
17	Shower	50	.1366	.2771	.4137	.3302	91.59	221.4	305	17.82	222.3	5692	1.251	17.82	
18	Shower	100	.1443	.2767	.4210	.3428	103.70	246.3	332	38.98	245.5	6266	1.265	38.98	
17	Shower-grid	100	.0828	.3543	.4371	.1894	93.65	214.3	307	116.79	229.0	5585	1.235	110.60	6.19
7	Shower-grid	100	.0745	.3962	.4707	.1582	89.66	190.5	290	116.90	211.1	4900	1.252	97.80	19.10
8	Shower-grid	100	.1350	.2497	.3847	.3510	102.4	266.2	325	134.69	274.0	6718	1.275	126.10	8.59

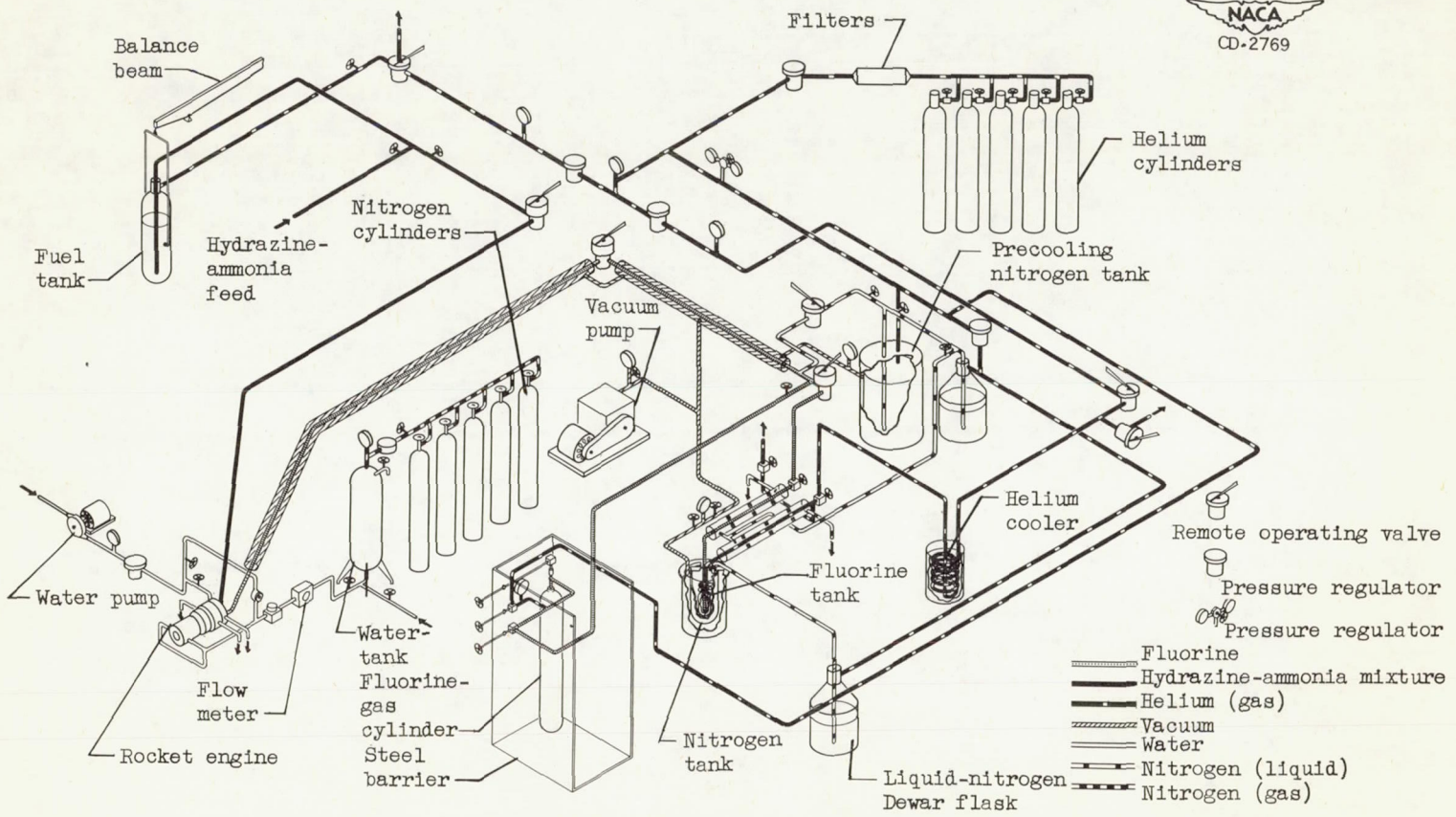
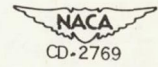


Figure 1. - Diagrammatic sketch of 100-pound-thrust rocket apparatus for investigation of liquid fluorine - hydrazine ammonia.

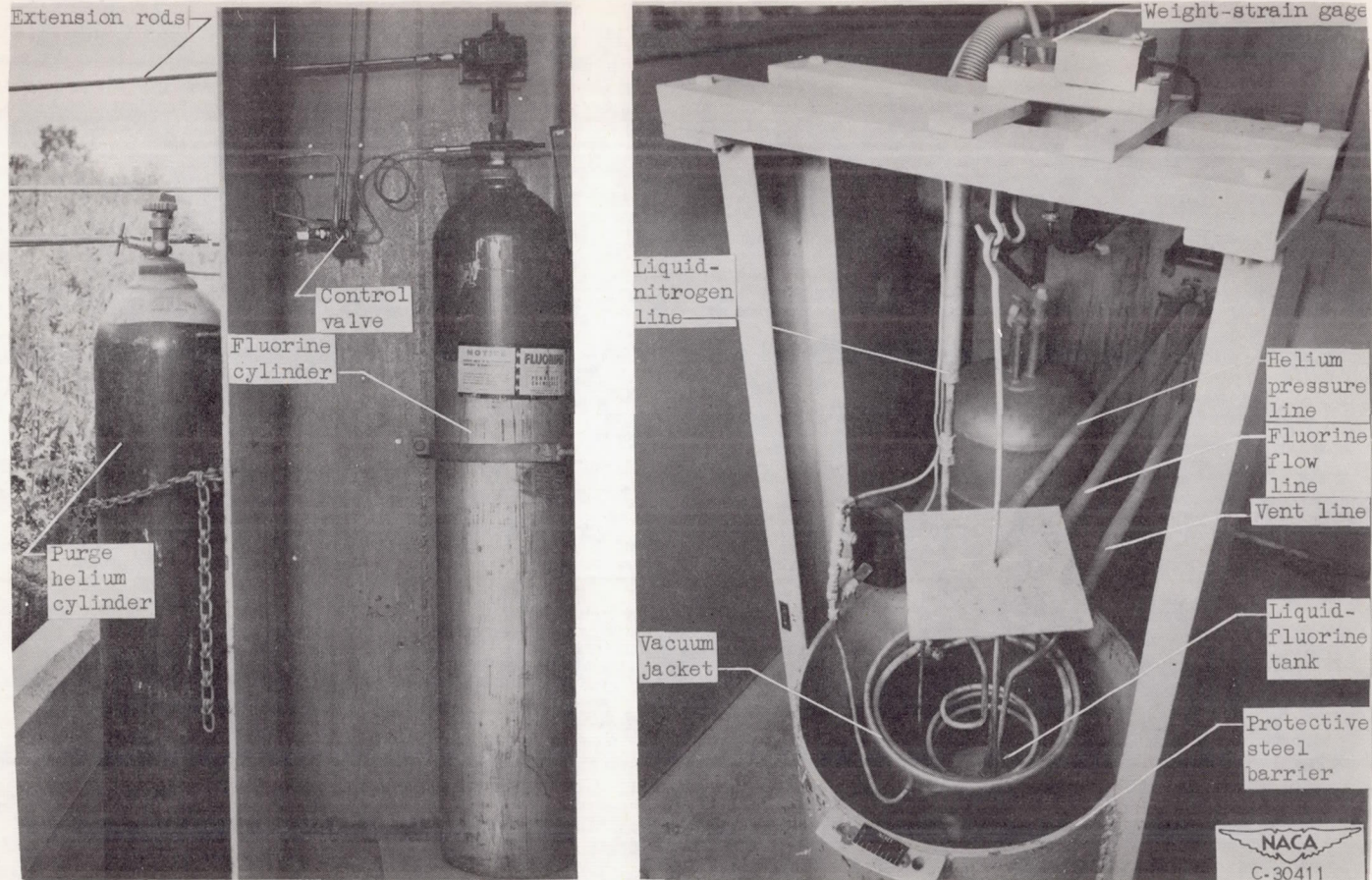


Figure 2. - Fluorine supply system for 100-pound-thrust fluorine - hydrazine-ammonia rocket engine.

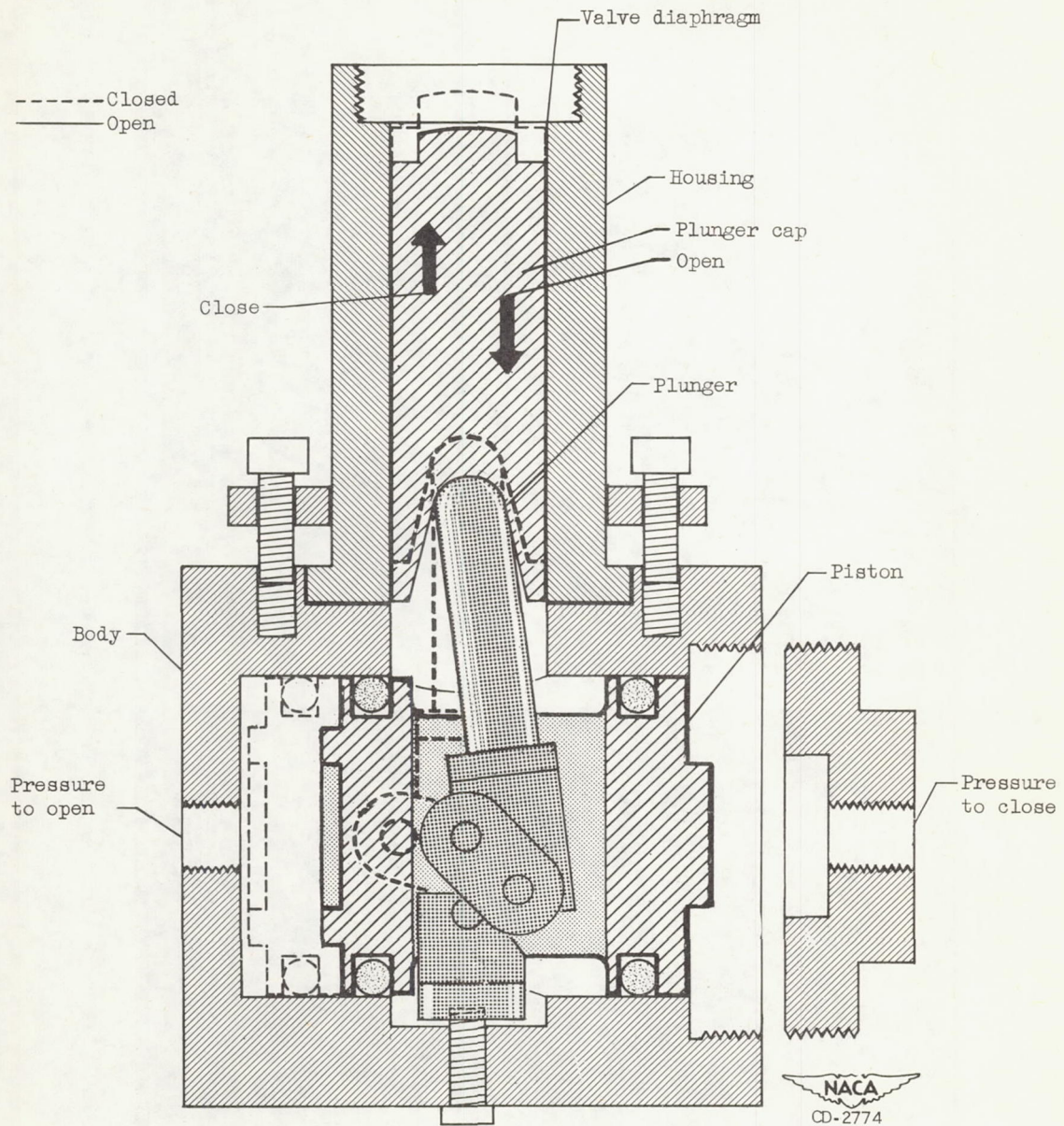


Figure 3. - Toggle actuator for fluorine valve.

2671

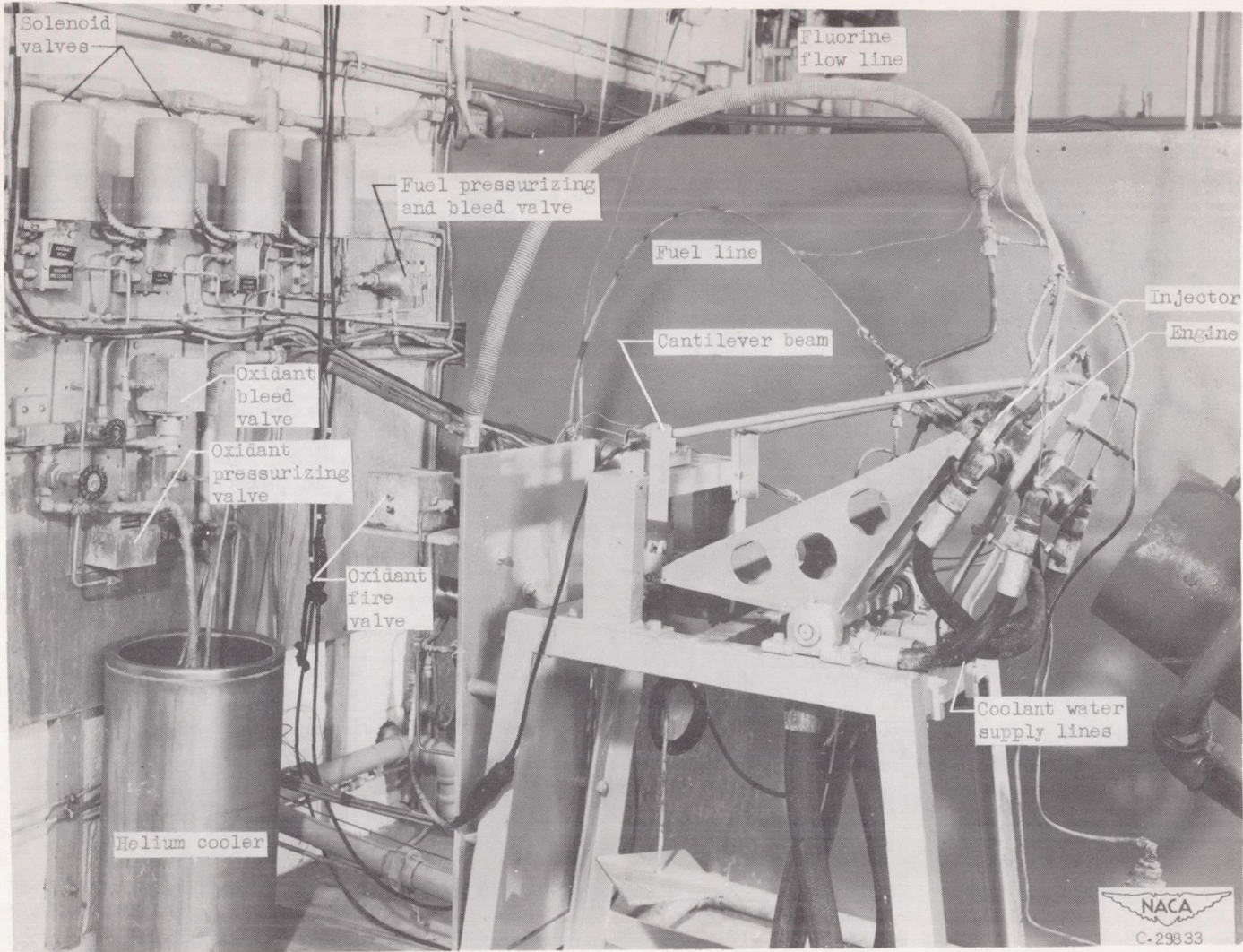
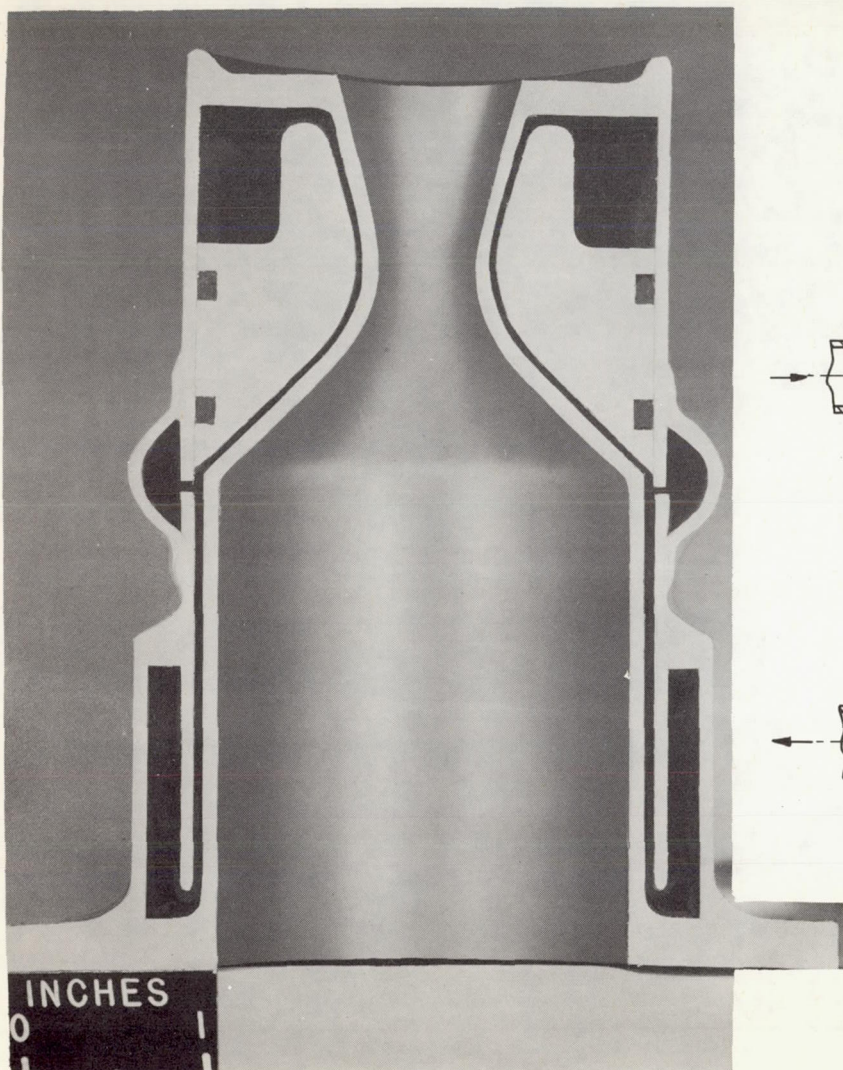
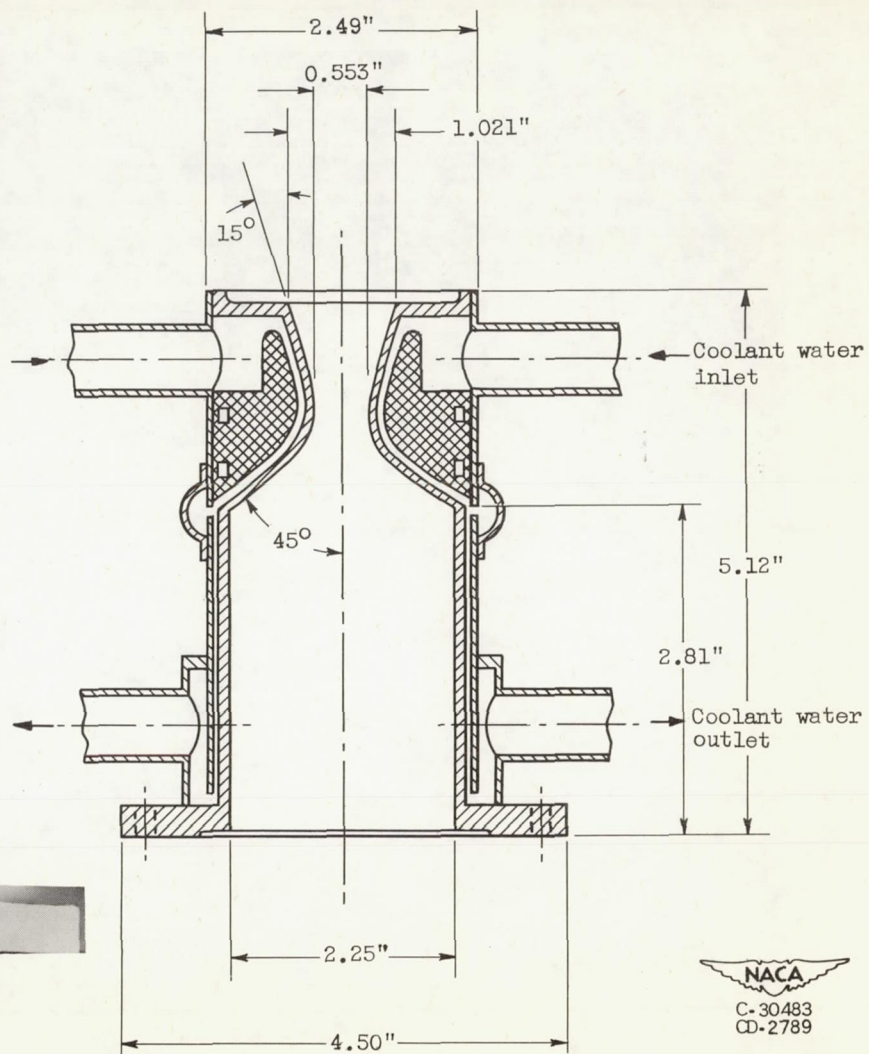


Figure 4. - Thrust stand for 100-pound-thrust fluorine - hydrazine-ammonia rocket engine.



(a) Section through combustion chamber and nozzle.



(b) Diagrammatic sketch.

Figure 5. - Combustion chamber and nozzle of 50 L* engine.

NACA
C-30483
CD-2789

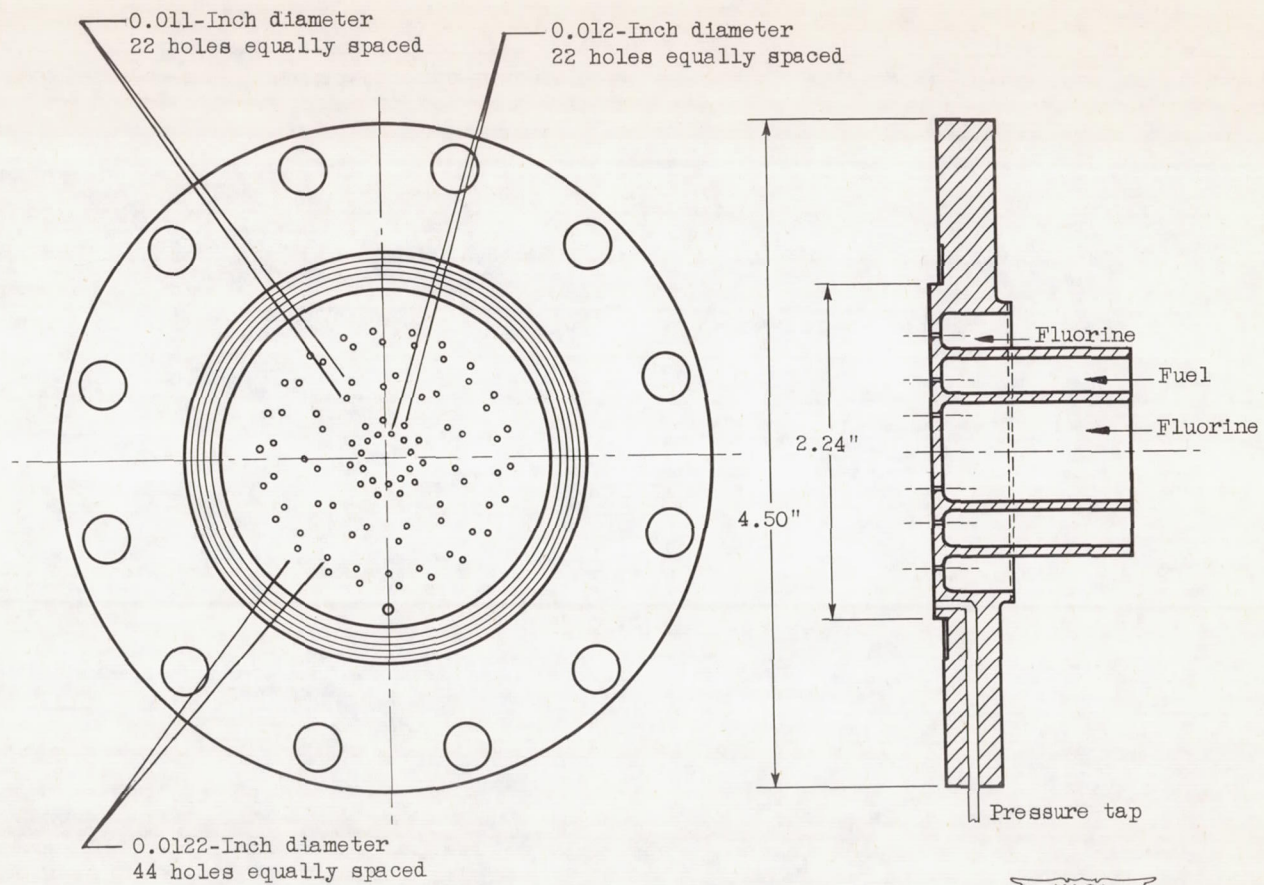


Figure 6. - Shower-head injector.

NACA
D-2770

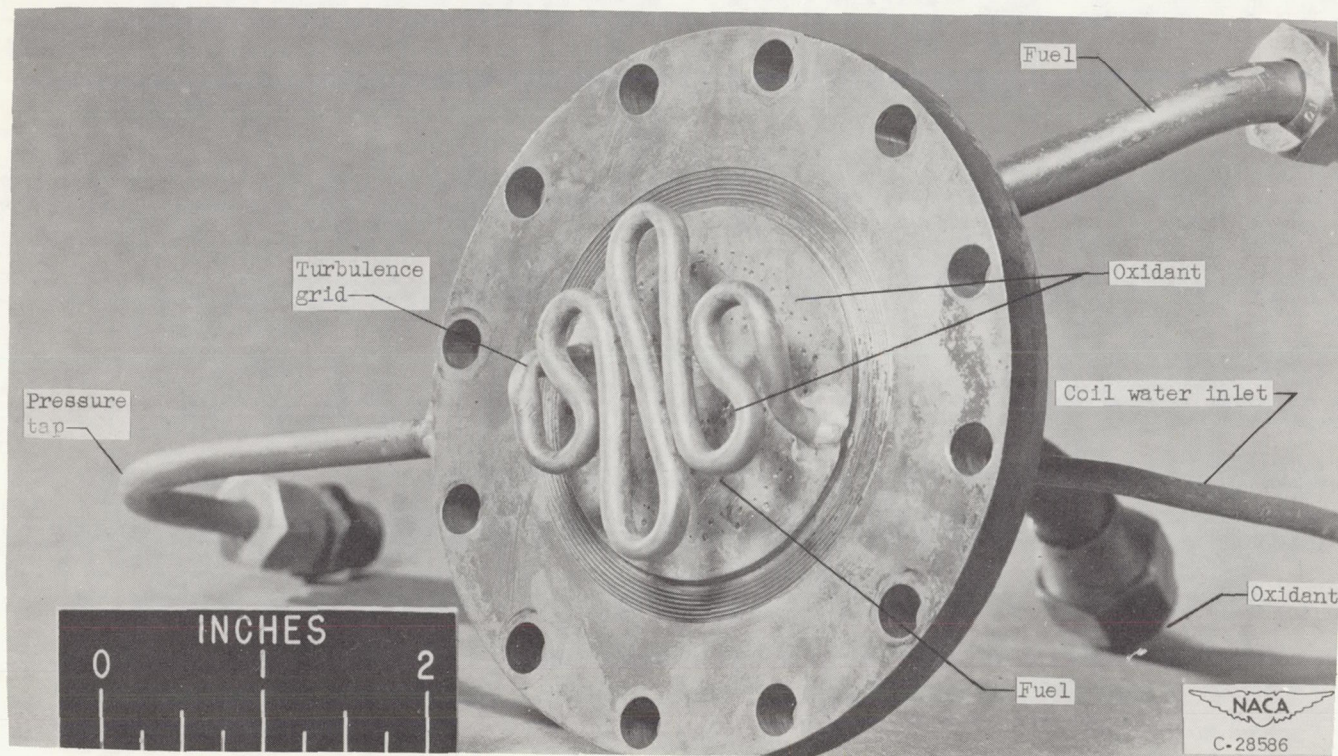


Figure 7. - Modified shower-head injector with water-cooled grid.

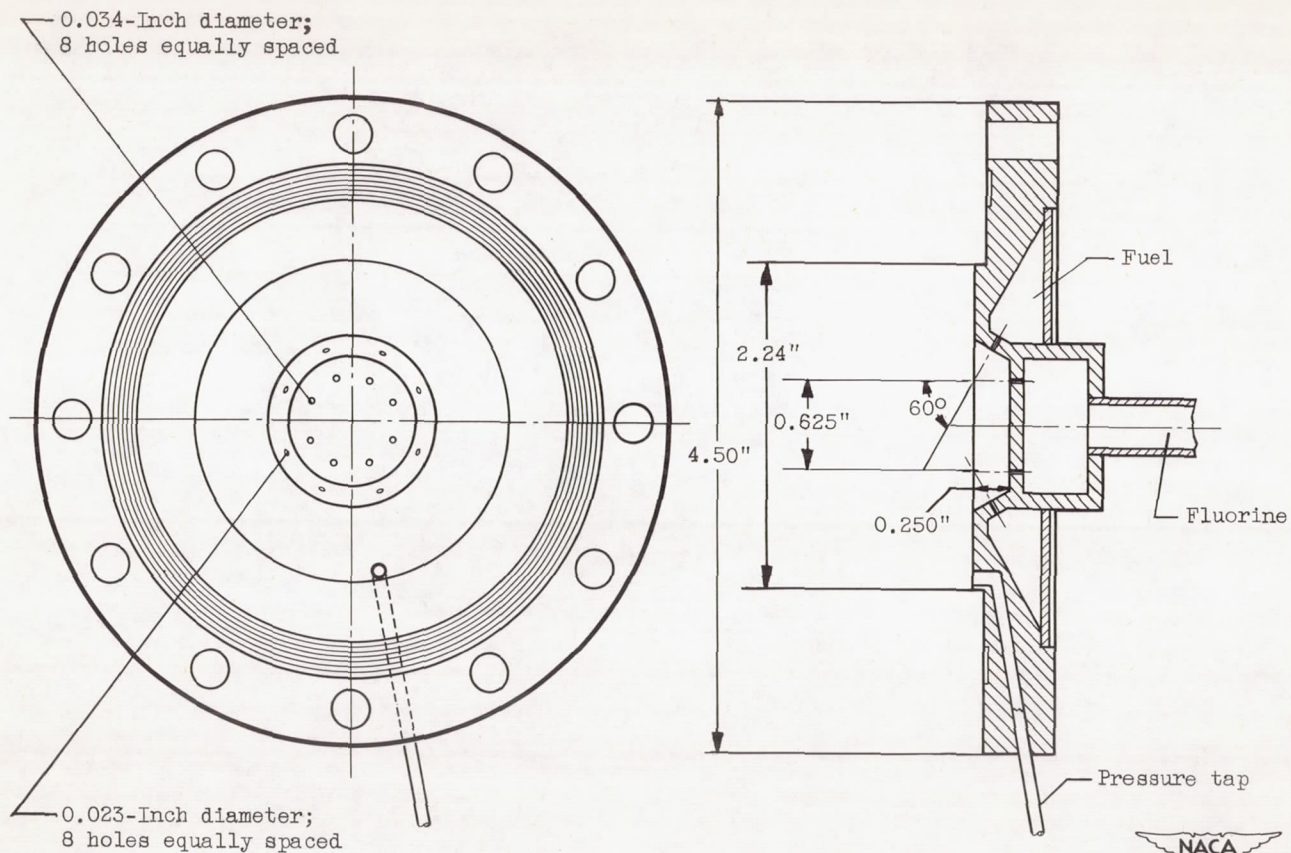


Figure 8. - Impinging-jet injector.

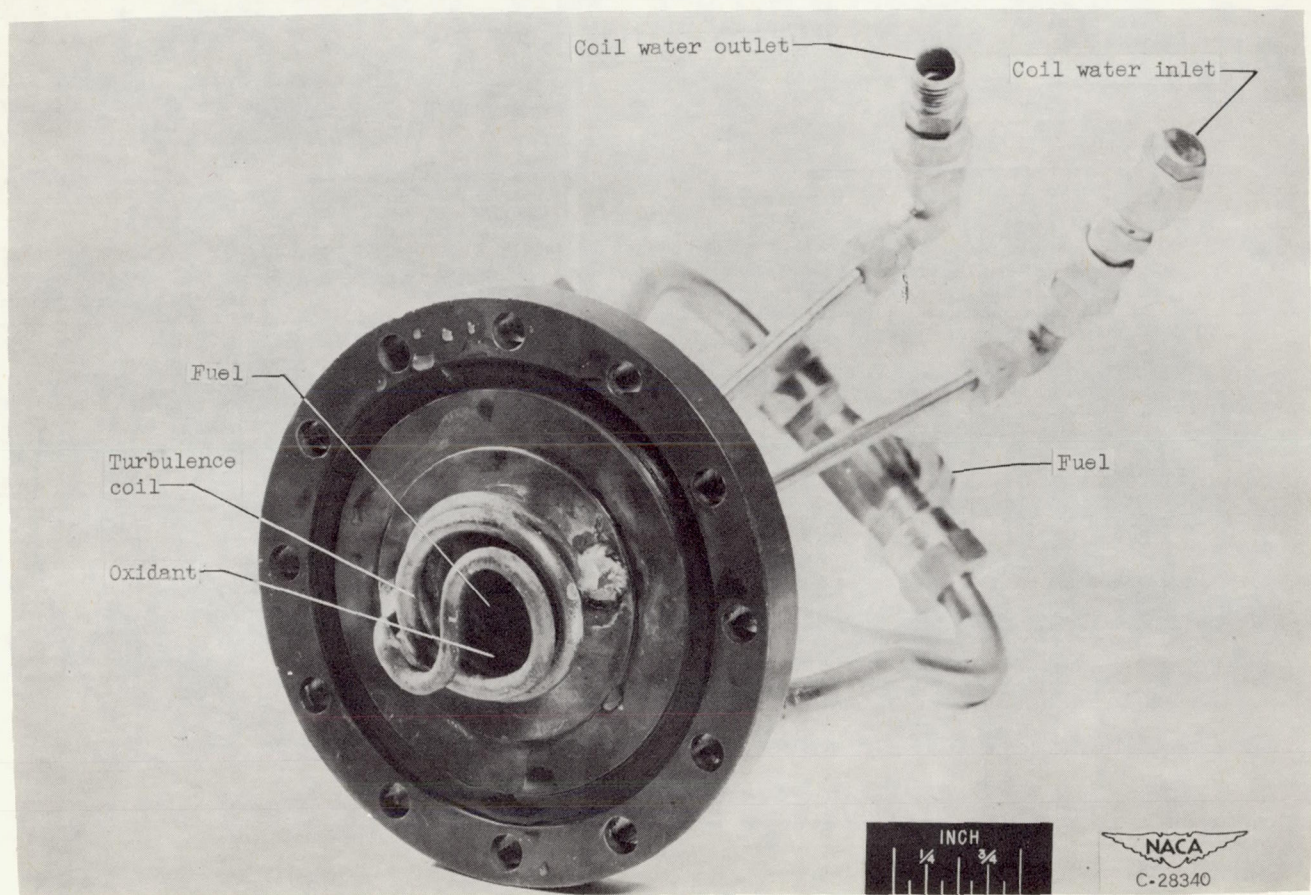


Figure 9. - One-to-one impinging-jet injector with turbulence coil A.

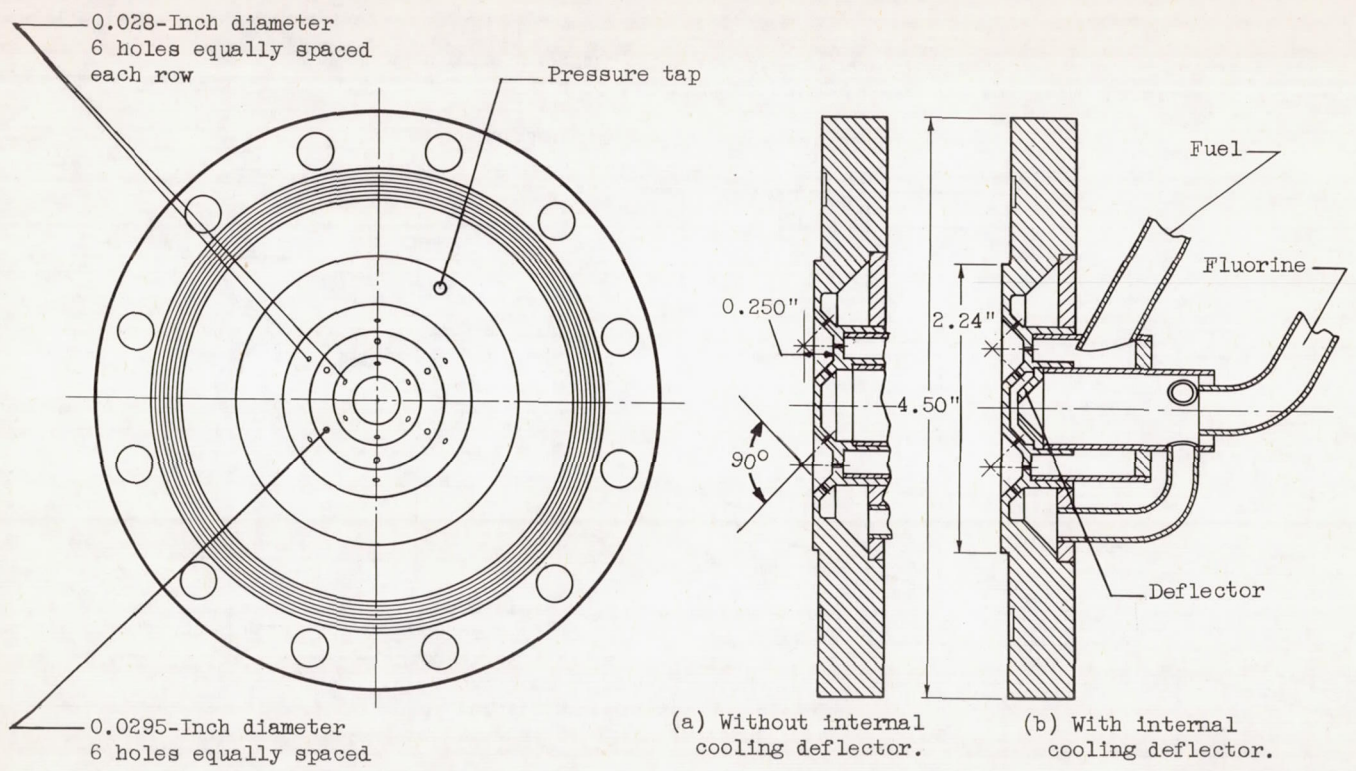
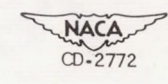


Figure 10. - Two oxidant - one fuel impinging-jet injector.



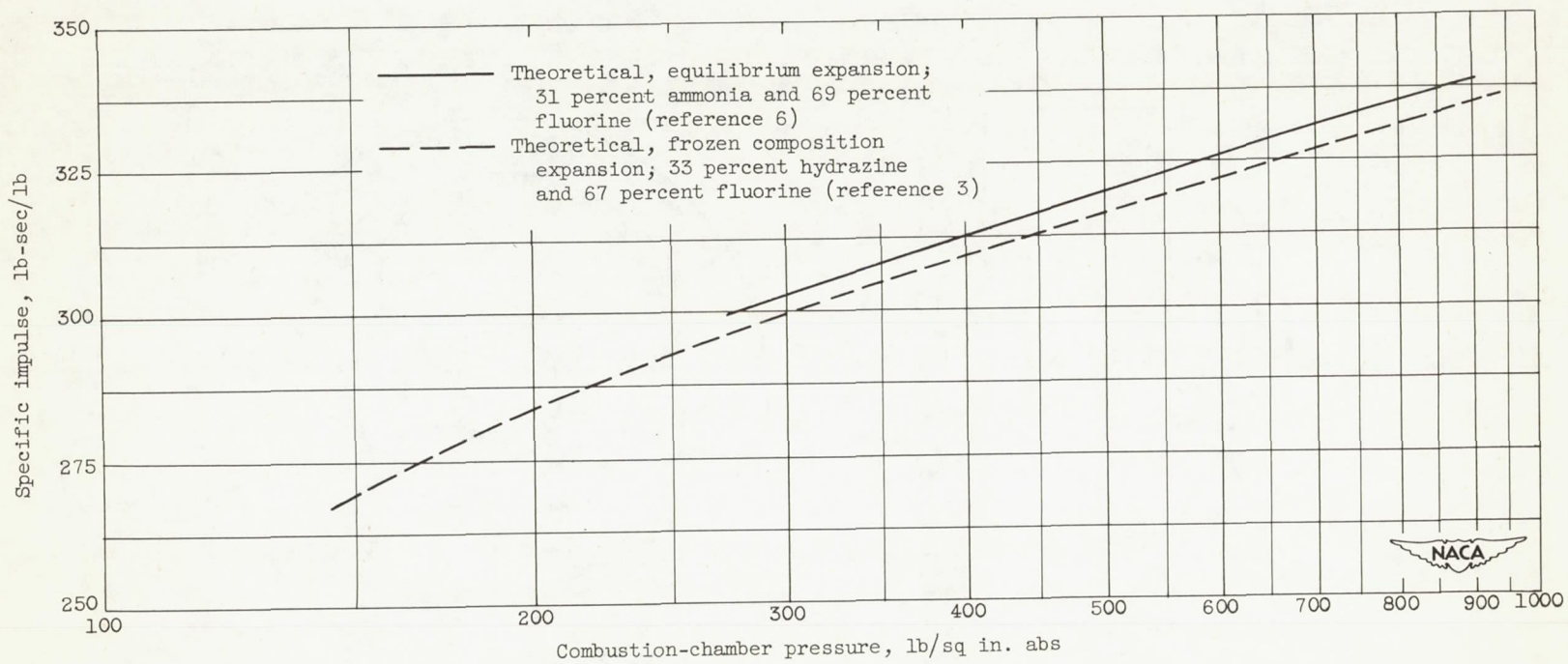
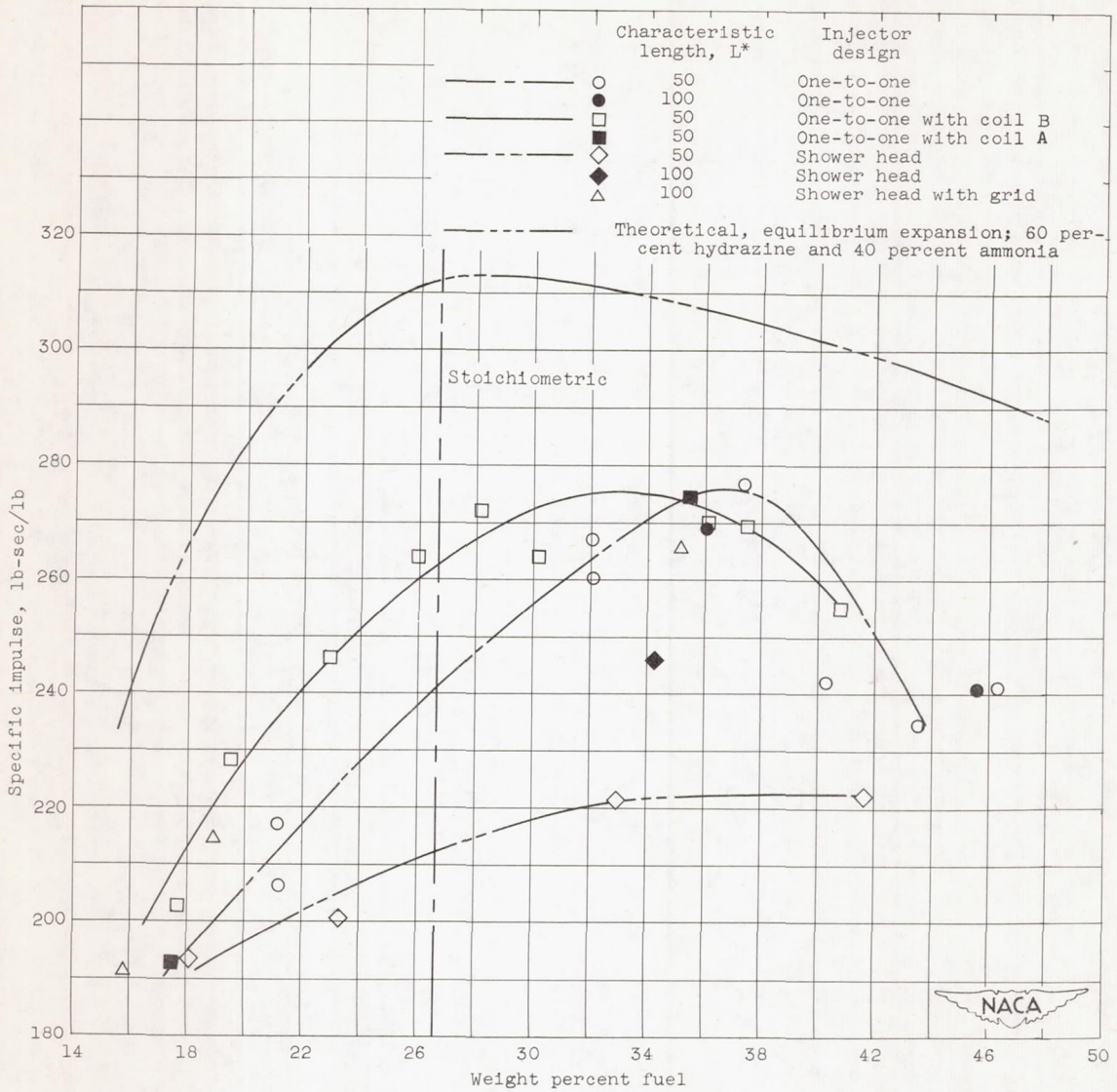


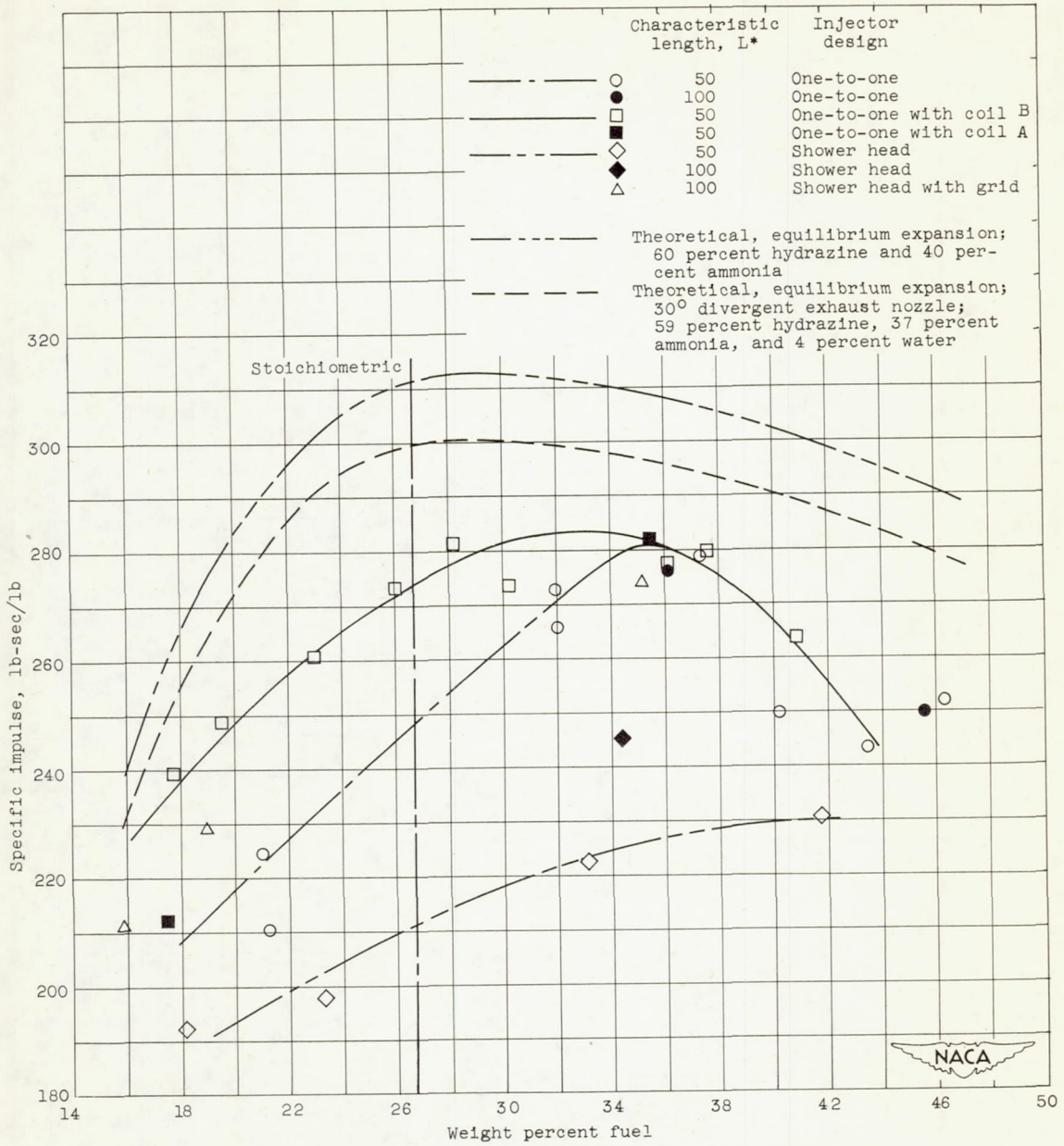
Figure 11. - Theoretical specific impulse of liquid fluorine with liquid ammonia and with hydrazine at various combustion-chamber pressures. $\Delta I_p \cong K \log p/P_c$ where $K = 88.65$.

2671



(a) Comparison of measured and calculated values.

Figure 12. - Theoretical and experimental specific impulse of liquid fluorine and hydrazine-ammonia fuel in 100-pound-thrust rocket engine.



(b) Comparison of corrected experimental and calculated values.

Figure 12. - Concluded. Theoretical and experimental specific impulse of liquid fluorine and hydrazine-ammonia fuel in 100-pound-thrust rocket engine.

T 107

2671

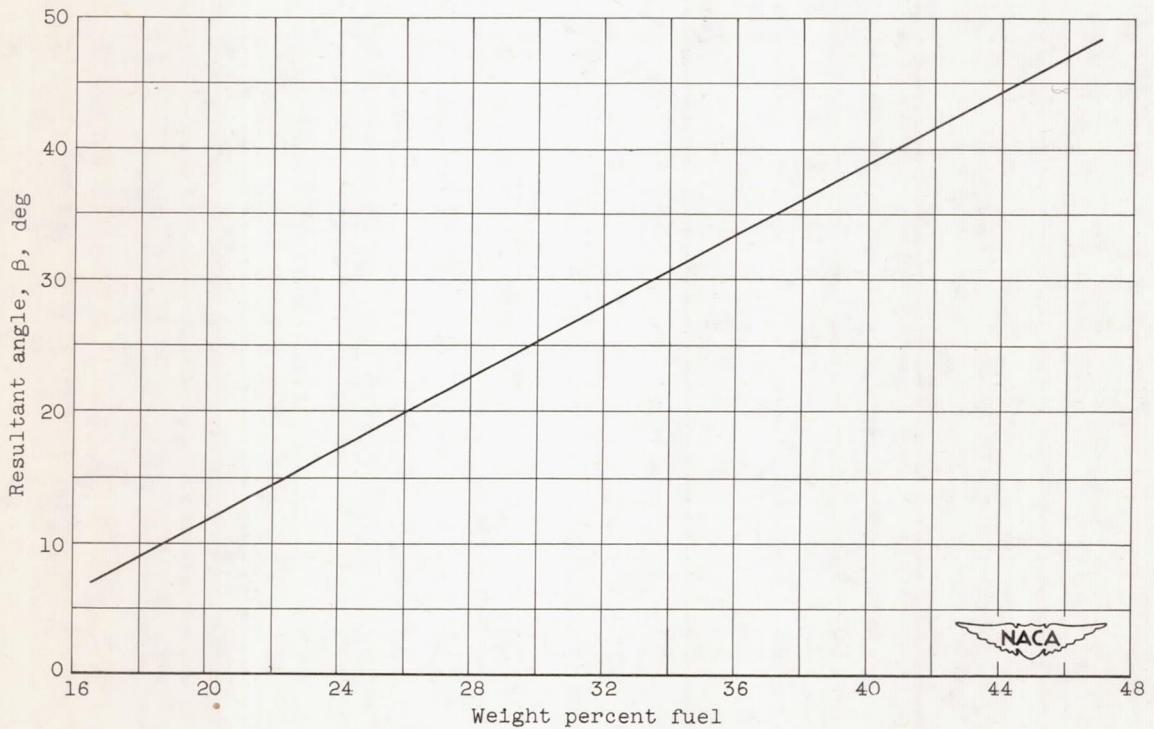
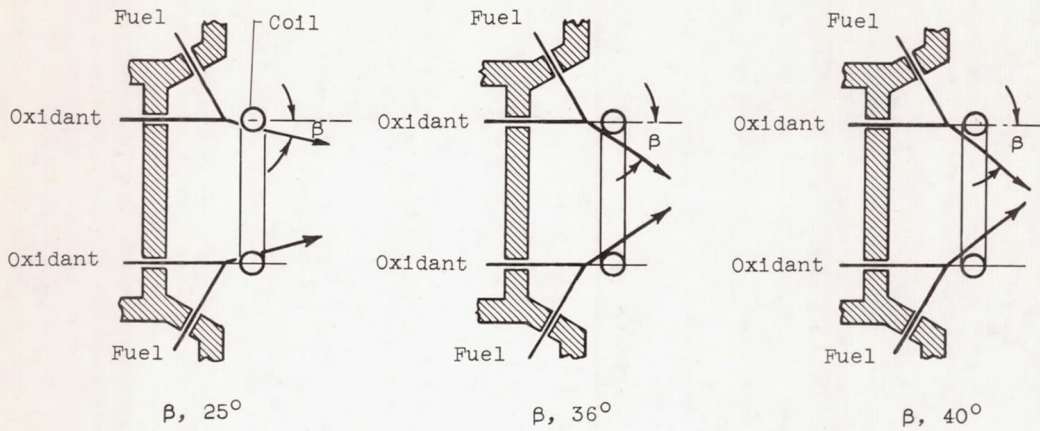
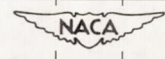


Figure 13. - Variation of angle of resultant stream with weight percent fuel for one-oxidant - one-fuel impinging-jet injector.



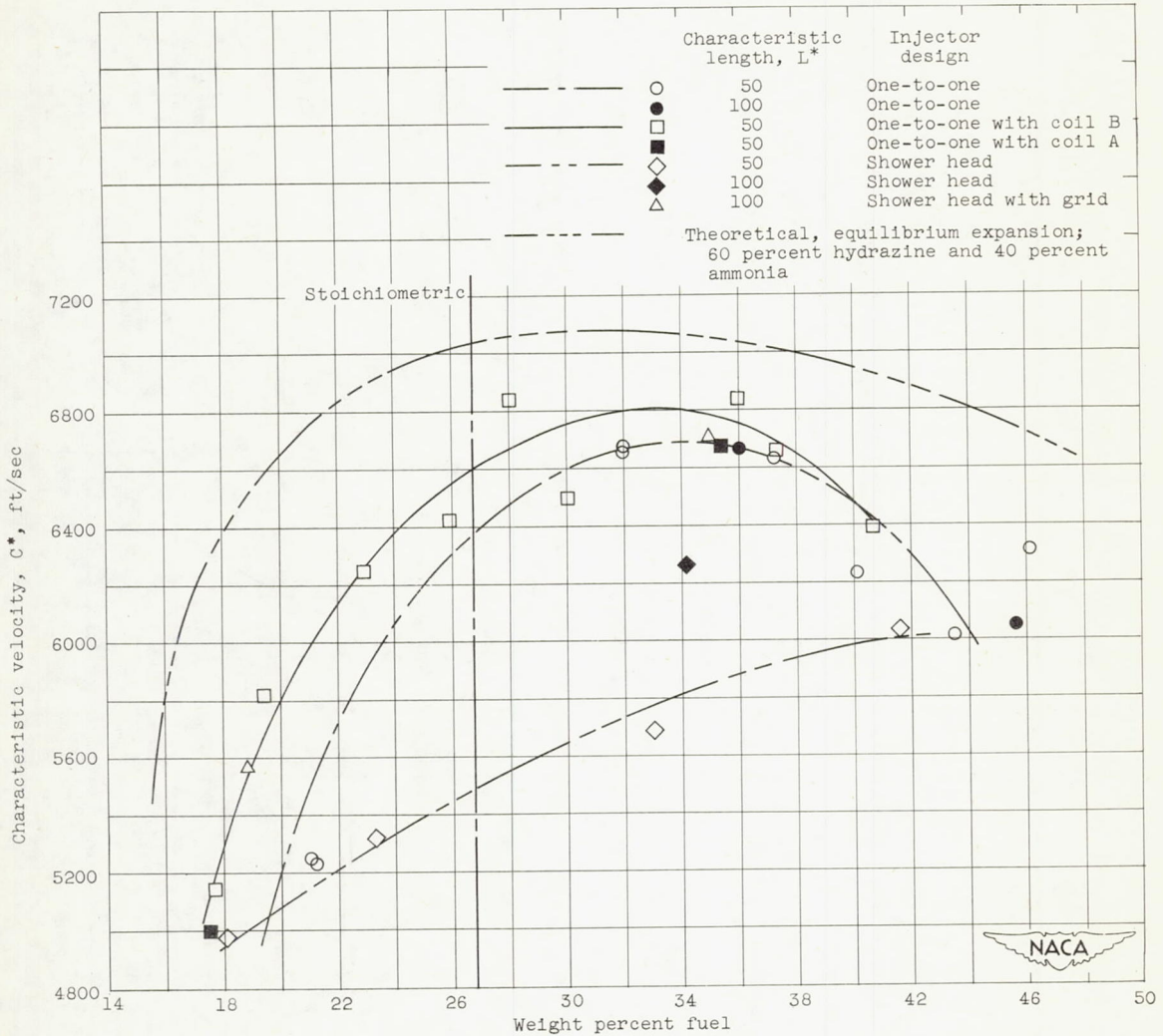


Figure 14. - Theoretical and experimental characteristic velocity of liquid fluorine and hydrazine-ammonia fuel in a 100-pound-thrust rocket engine.



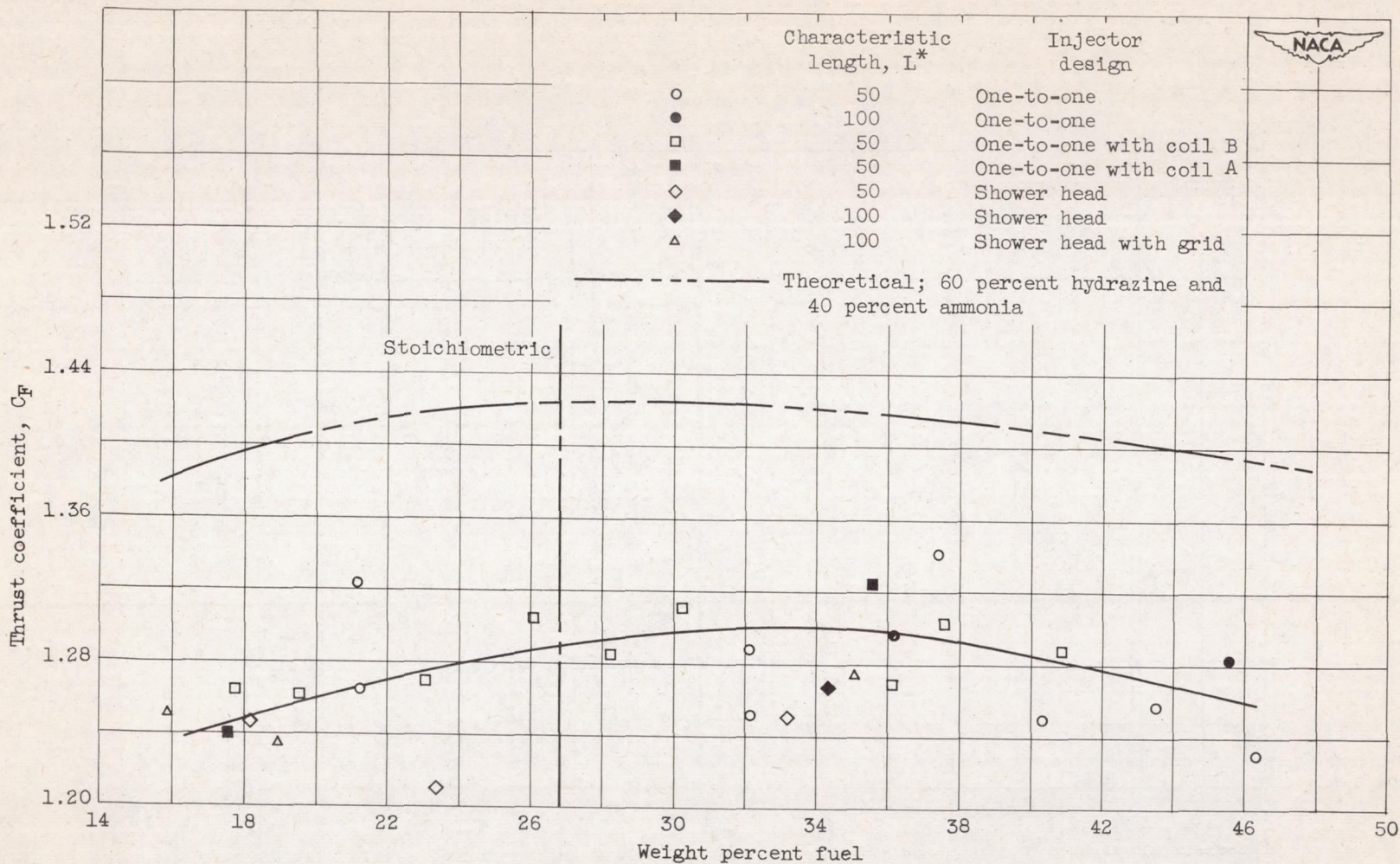
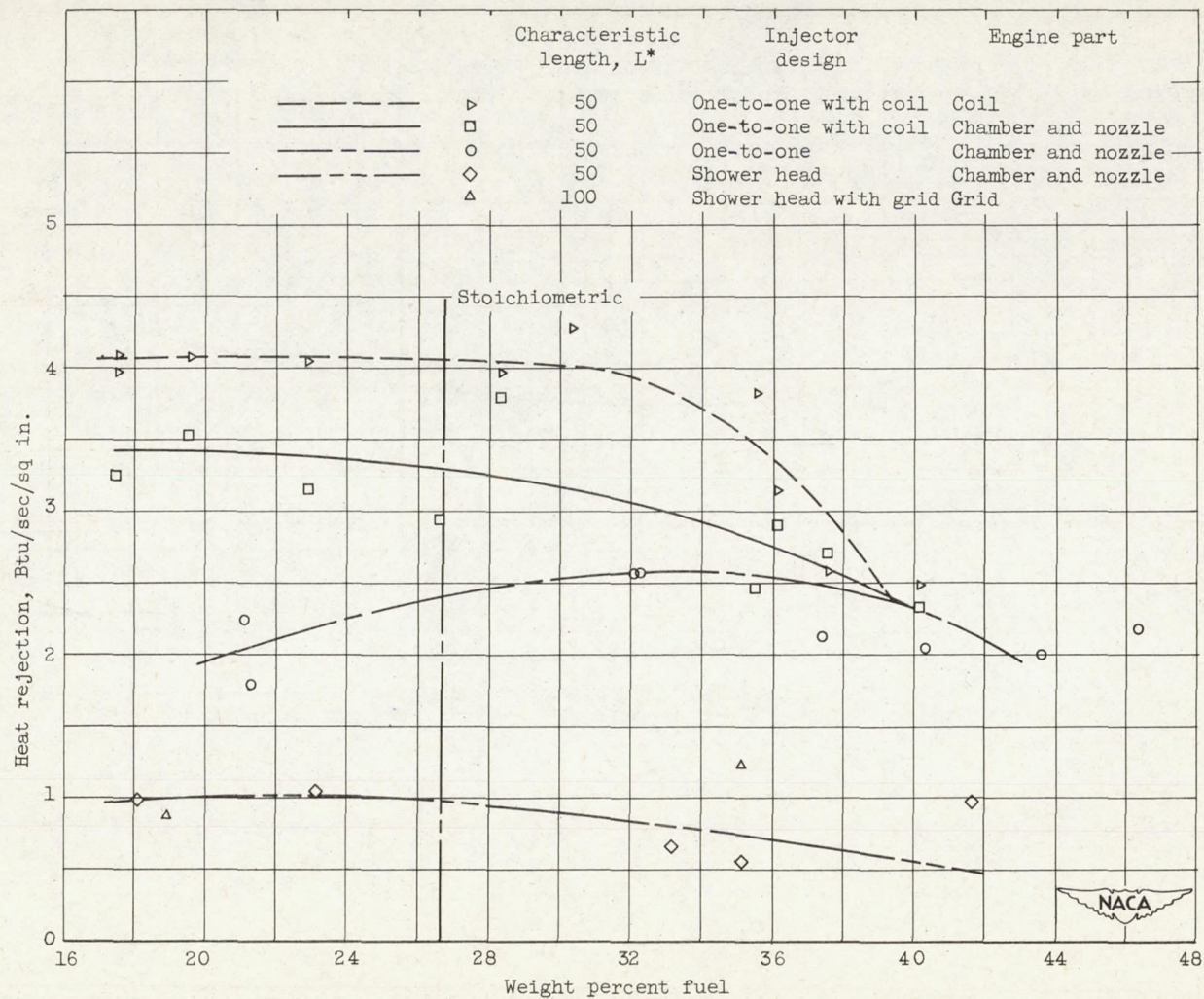
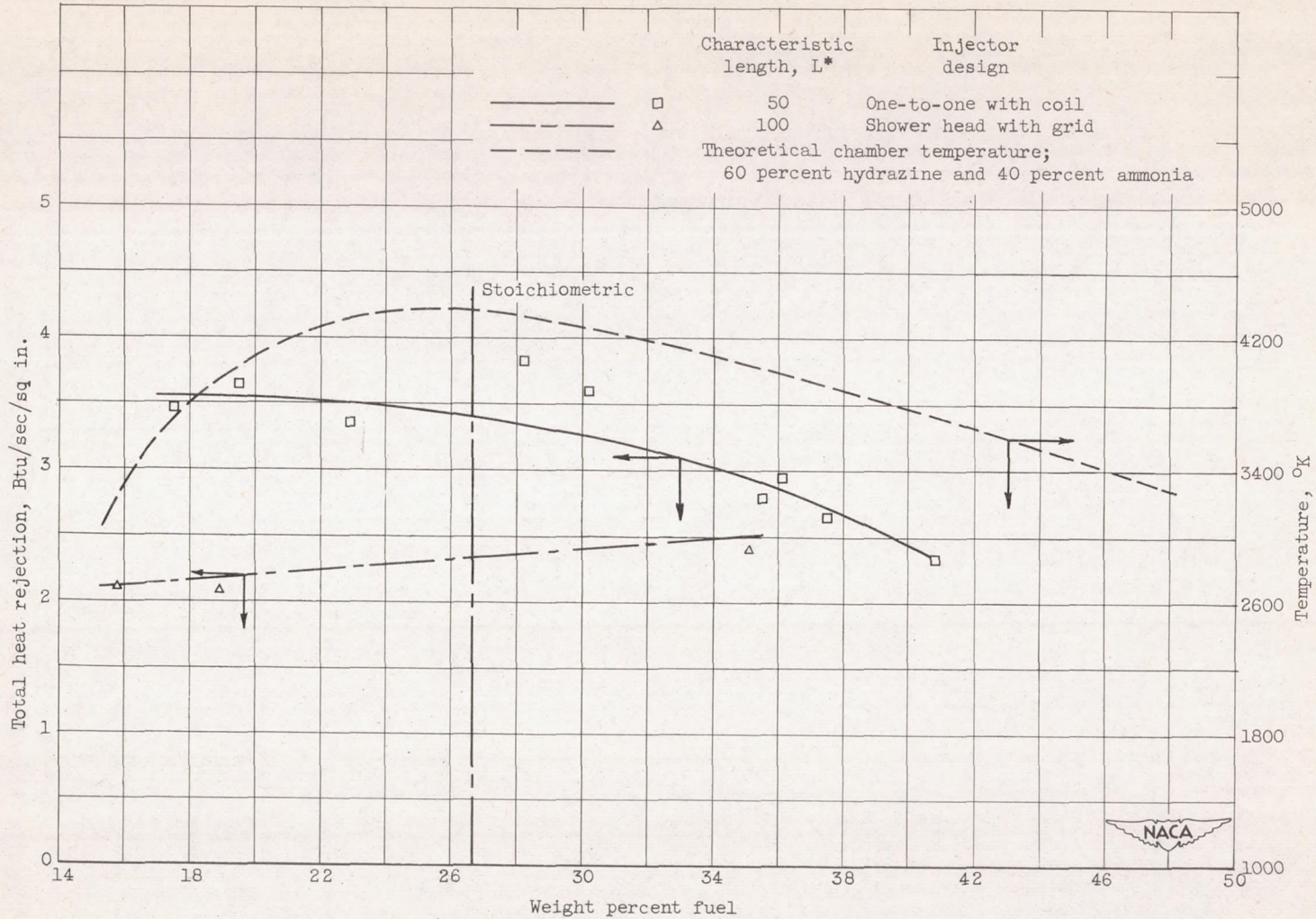


Figure 15. - Theoretical and experimental thrust coefficient of liquid fluorine and hydrazine-ammonia fuel in 100-pound-thrust rocket engine.



(a) Heat rejection to engine parts.

Figure 16. - Heat rejection of liquid fluorine and hydrazine-ammonia fuel in a 100-pound-thrust rocket engine.



(b) Heat rejection to complete engine configuration and theoretical chamber temperature.

Figure 16. - Concluded. Heat rejection of liquid fluorine and hydrazine-ammonia fuel in a 100-pound-thrust rocket engine.

